

**JIMMA UNIVERSITY**  
**SCHOOL OF GRADUATE STUDIES**  
**DEPARTMENT OF CHEMISTRY**



**STUDY ON FABRICATION OF RANDOMLY NANO ARRAYED  
ELECTRODES AND THEIR APPLICATIONS IN ELECTROANALYSIS**

**By: BIKILA NAGASA**

**ADVISOR: TESFAYE REFERA (Ph.D)**

**CO-ADVISOR: SHIMELES ADDISU (M.Sc.)**

**DECEMBER, 2012**

**JIMMA, ETHIOPIA**

**STUDY ON FABRICATION OF RANDOMLY NANO ARRAYED  
ELECTRODES AND THEIR APPLICATIONS IN ELECTROANALYSIS**

**By**

**BIKILA NAGASA**

**ADVISOR: TEFAYE REFERA (Ph.D)**

**CO-ADVISOR: SHIMELES ADDISU (M.Sc.)**

**A THESIS SUBMITTED TO SCHOOL OF GRADUATE STUDIES, JIMMA  
UNIVERSITY IN PARTIAL FULFILLMENT OF THE REQUIREMENTS  
FOR THE DEGREE OF MASTERS OF SCIENCE IN CHEMISTRY  
(ANALYTICAL CHEMISTRY)**

**DECEMBER, 2012**

Study on Fabrication of Randomly Nano Arrayed Electrodes and Their  
Applications in Electroanalysis

By: Bikila Nagasa

A Thesis Submitted to the School of Graduate Studies, Jimma University in Partial  
Fulfillment of the Requirements for the Degree of Masters of Science in Chemistry  
(Analytical Chemistry)

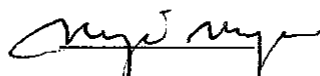
**Approved by Board of Examiners**

**Signature**

**Date**

**External examiner**

Negussie Megersa



Dec. 15, 2012

**Internal examiner**

\_\_\_\_\_

\_\_\_\_\_

\_\_\_\_\_

**Advisors**

\_\_\_\_\_

\_\_\_\_\_

\_\_\_\_\_

\_\_\_\_\_

\_\_\_\_\_

\_\_\_\_\_

**Department Head**

\_\_\_\_\_

\_\_\_\_\_

\_\_\_\_\_

## Table of Contents

Contents	pages
Table of Contents .....	i
List of Figures .....	v
List of Schemes .....	viii
List of Tables .....	x
List of Abbreviation .....	xi
Acknowledgements .....	xii
Abstract .....	xiii
1 Introduction .....	1
1.1 Electroanalysis .....	1
1.2 Chemically Modified Electrodes and Their Applications .....	1
1.3 Literature Review .....	3
1.3.1 Electrode Surface Modification .....	3
1.3.2 Self Assembled Monolayer Strategies .....	4
1.3.3 Grafting of Diazonium Salts on Glassy Carbon Electrode .....	5
1.3.4 Nanostructuring of Electrodes .....	7
1.3.5 Electrochemical Detection of Dopamine and Ascorbic Acid .....	9
1.4 Theoretical Background .....	11
1.4.1 Electrochemical Cell .....	11
1.4.2 Voltammetric Techniques .....	11
1.4.3 Nanotechnology and Nanoparticles .....	14
1.4.4 Deposition of Metal Nanoparticles .....	15
1.4.5 Microelectrodes and Nanoelectrodes .....	16
1.4.6 Geometry of Nanoelectrodes .....	17
1.4.7 Mass Transport to Nanoelectrodes .....	18

1.5 Statement of the Problem .....	19
1.6 Hypothesis .....	19
1.7 Objectives of the Study .....	20
1.7.1 General Objective .....	20
1.7.2 Specific Objectives .....	20
2 Materials and Methods.....	20
2.1 Electrochemical Measurement .....	20
2.2 Chemicals and Reagents.....	21
2.3 Experimental Procedures.....	21
2.3.1 Electrode Pretreatment.....	21
2.3.2 Fabrication of Randomly Nanoarrayed Electrodes.....	22
2.3.3 Electrochemical Characterization of Randomly Nanoarrayed Electrodes.....	24
2.3.4 Preparation of Ascorbic Acid Solutions .....	24
2.3.5 Preparation of Dopamine Solution.....	24
2.3.6 Preparation of Solutions of Interferents.....	25
2.3.7 Analysis of Real Samples .....	25
3 Results and Discussion .....	27
3.1 Electrodeposition of Gold Nanoparticles .....	27
3.2 Grafting Diazonium Salts on Glassy Carbon Electrode .....	28
3.2.1 Grafting of 4-Aminophenol Film.....	29
3.2.2 Grafting of P-Phenylenediamine Film .....	30
3.2.3 Grafting p-Nitroaniline Film.....	31
3.3 Electrochemical Characterization of 4-aminophenol Grafted Nanostructure GCE .....	33
3.3.1 Cyclic Voltammetry of $\text{Ru}(\text{NH}_3)_6\text{Cl}_3$ .....	33
3.3.2 Cyclic Voltammetry of $\text{K}_3\text{Fe}(\text{CN})_6$ .....	34
3.3.3 Cyclic Voltammetry of Hydroquinone .....	35

3.3.4 Investigation of Mass Transport of Redox Probes Towards Modified Electrodes .	35
3.4 Determination of Ascorbic acid at 4-Aminophenol Grafted Nanostructured Glassy	
Carbon Electrode.....	38
3.4.1 Effect of pH on Oxidation Peak Current of Ascorbic Acid.....	39
3.4.2 Amperometric Response of Ascorbic Acid .....	41
3.4.3 Effect of Interferent.....	43
3.4.4 Real Sample Analysis .....	44
3.5 Stability and Reproducibility of Nanohole 4-Aminophenol Grafted Glassy Carbon Electrode	
.....	45
3.6 Electrochemical Characterization of p-Phenylenediamine Grafted Nanostructure Glassy	
Carbon Electrode.....	46
3.6.1 Cyclic Voltammetry of $\text{Ru}(\text{NH}_3)_6\text{Cl}_3$ .....	46
3.6.2 Cyclic Voltammetry of $\text{K}_3\text{Fe}(\text{CN})_6$ .....	47
3.6.3 Cyclic Voltammetry of Hydroquinone .....	48
3.6.4 Effect of Scan Rate on Oxidation Peak Current of $\text{K}_3\text{Fe}(\text{CN})_6$ and Hydroquinone	
Probes .....	49
3.7 Determination of Ascorbic Acid at p-Phenylenediamine Grafted Nanostructured Glassy	
Carbon Electrode.....	51
3.7.1 Effect of pH on Oxidation Peak Current of Ascorbic Acid.....	53
3.7.2 Amperometric Response of Ascorbic Acid .....	55
3.7.3 Effect of Interferent.....	57
3.7.4 Real sample Analysis.....	58
3.7.5 Stability and Reproducibility of Nanohole p-Phenylenediamine Grafted Glassy	
Carbon Electrode.....	59
3.8 Electrochemical Characterization of p-Nitroaniline Grafted Nanostructured Glassy Carbon	
Electrode.....	60
3.8.1 Cyclic Voltammetry of $\text{K}_3\text{Fe}(\text{CN})_6$ .....	60

3.8.2 Cyclic Voltammetry of Ru(NH <sub>3</sub> ) <sub>6</sub> Cl <sub>3</sub> .....	61
3.8.3 Cyclic Voltammetry of Hydroquinone .....	62
3.8.4 Effect of Scan Rate on Oxidation Peak Current of Ru (NH <sub>3</sub> ) <sub>6</sub> Cl <sub>3</sub> and Hydroquinone .....	62
3.8.5 Cyclic Voltammetry of Dopamine.....	65
4 Conclusion and Future Prospective .....	74
Reference .....	75

## List of Figures

Figures	pages
Figure 1. Self-assembled monolayers of thiols on gold.....	5
Figure 2. Molecular structure of ascorbic acid. ....	9
Figure 3. Molecular structure of dopamine.....	9
Figure 4 Potential-time stimulation signal of the cyclic voltammetry.....	12
Figure 5. Nanoelectrode geometries: hemispherical electrode, inlaid disc electrode and recessed disc electrode; diffusion modes and the equations for the corresponding steady-state currents .....	17
Figure 6. Cyclic voltamogram of 0.1 mmol/L $\text{KAuCl}_4$ in 0.5 mol/L $\text{H}_2\text{SO}_4$ ; Inset reduction of a gold oxide layer formed at a scan rate of 50 mV/s .....	27
Figure 7. Cyclic voltamogram of grafting of 3 mmol/L 4-aminophenol (A) at bare GCE and (B) at AuNPs deposited GCE in 0.5 mol/L HCl ( $v=100$ mV/s) (C) Cyclic voltamogram of AuNPs nucleated 4-aminophenol modified GCE in 0.1 mol/L KCl ( $v = 100$ mV/s) for 3 cycles (1, 2, 3 representing first cycle, second cycle and third cycle respectively) .	29
Figure 8. Cyclic voltamogram of grafting of 3 mmol/L p-phenylenediamine in 0.5 mol/L HCl at (A) bare GCE and (B) AUNPS deposited GCE in 0.1 mol/L KCl; (C) Cyclic voltamogram of AUNPS nucleated p-phenylenediamine modified GCE for 3 cycles (1, 2 and 3 representing first cycle, second cycle and third cycle, respectively) in all cases scan rate 100 mV/s .....	31
Figure 9. Cyclic voltamogram of grafting of 3 mmol/L p-nitroaniline on (A) bare GCE and (B) AuNPs deposited GCE in 0.5 mol/L HCl ( C ) Cyclic voltamogram of AuNPs nucleated PD modified GCE in 0.1 mol/L KCl for 3 cycles (1, 2, 3 represent first cycle, second cycle and third cycle) in all cases scan rate 100 mV/s.....	32
Figure 10. Cyclic voltamogram of 10 mmol/L $\text{Ru}(\text{NH}_3)_6\text{Cl}_3$ in 0.1 mmol/L $\text{KNO}_3$ ; (a) at bare GCE (b) Aph grafted GCE (c) nanohole Aph grafted GCE; inset cyclic voltamogram of supporting electrolyte ( 0.1 mol/L $\text{KNO}_3$ ) at nanohole Aph grafted GCE in all cases scan rate 50 mV/s .....	33



Figure 11. Cyclic voltamogram of 10 mmol/L $K_3Fe(CN)_6$ in 0.1 mol/L KCl at 50 mv/s; (a) at nanohole Aph grafted GCE (b) Aph grafted GCE (C) bare GCE Inset CV of 0.1 KCl; inset cyclic voltamogram of supporting electrolyte (0.1 mol/l KCl ) at nanohole Aph grafted GCE in all cases scan rate 50 mV/s.....	34
Figure 12. Cyclic voltamogram of 10 mmol/L HQ in 0.1 mol/L $NaClO_4$ ; (a) at nanohole Aph grafted GCE (b) bare GCE and (c) Aph grafted GCE; inset cyclic voltamogram of supporting electrolyte (0.1 mol/L $NaClO_4$ ) at nanohole Aph grafted GCE in all cases scan rate 100 mV/s.....	35
Figure 13. Cyclic voltamogram of 2 mmol/L AA at (a) bare and (b) nanohole Aph grafted GCE in 0.1 mol/L sodium acetate buffer solution; inset Cyclic voltamogram of 0.1 mol/L sodium acetate buffer solution (pH 5) at nanohole Aph grafted GCE in all cases scan rate 100 mV/s.....	39
Figure 14. Oxidation peak current of 2 mmol/L AA at different pH at (a) bare GCE (b) nanohole Aph grafted GCE .....	40
Figure 15. Amperometric calibration curve for determination of AA in acetate buffer ( pH 5) at ( i ) bare GC; (ii) nanohole Aph grafted GCE.; inset (A) amperometric current vs time curve upon successive additions of 1m mol/L AA into a stirred system of 0.1 mol/L sodium acetate buffer (B) amperometric response of buffer only ( pH 5) .....	42
Figure 16. Amperometric response of 2 mmol/L AA and 200-fold excesses of interfering species, Inset: Amperometric response from interferent to AA at nanohole Aph grafted GCE at applied potential of 0.250 V .....	43
Figure 17. Cyclic Voltamogram of 10 mmol/L $Ru(NH_3)_6Cl_3$ in 0.1mol/L $KNO_3$ at 50 mv/s; inset Cyclic voltamogram of 0.1 mol/L $KNO_3$ .....	46
Figure18. Cyclic Voltamogram of 10 mmol/L $K_3Fe(CN)_6$ in 0.1 mol/L KCl at scan rate of 50 mv/s; Inset CV of 0.1 mol/L KCl .....	47
Figure 19. Cyclic voltamogram of 10 mmol/L HQ in 0.1 mol/L $NaClO_4$ at (a) bare GCE, (b) nanohole PD grafted GCE, (c) PD grafted GCE; Inset cyclic voltamogram of supporting electrolyte ( 0.1 mol/L $NaClO_4$ ), scan rate 100 mV/s in all cases.....	48

Figure 20. Cyclic voltamogram of 2 mmol/L AA in 0.1 mol/L sodium acetate buffer solution at 100 mV/s; inset Cyclic voltamogram of 0.1 mol/L sodium acetate buffer (pH 5).....	52
Figure 21. Cyclic voltamogram of 2 mmol/L AA in 0.1 mol/L sodium acetate buffer solution at pH 5 at 100 mV/s.....	53
Figure 22. Calibration curve of oxidation peak current of AA at different pH at nanohole PD grafted GCE. ....	54
Figure 23. Calibration curve of amperometric response of 2 mmol/L AA at nanohole PD grafted GC; inset (A) amperometric current vs. time curve upon successive additions of 1 mmol/L AA into a stirred system of 0.1 mol/L sodium acetate buffer (pH5) (B) amperometric current vs. time curve buffer only (pH 5).....	56
Figure 24. Amperometric response of (A) 1 mmol/L AA and mmol/L interfering species at bare GCE at 0.8 V (B) 1 mmol/L AA and 200-fold excesses of interfering species at nanohole PD grafted GCE at 0.237 V; (C) amperometric response of 1 mmol/L AA and 200-fold excesses of interfering species from interferent to AA at nanohole PD grafted GCE at 0.237 V. ....	57
Figure 26. Cyclic Voltamogram of 10 mmol/L Ru (NH <sub>3</sub> ) <sub>6</sub> Cl <sub>3</sub> in 0.1 mol/L KNO <sub>3</sub> ; at (a) nanohole PNA grafted GCE, (b) PNA grafted GCE, (c) bare GCE; Inset Cyclic voltamogram of nanohole PNA grafted GCE in blank supporting electrolyte (0.1 mol/L KNO <sub>3</sub> ) at 50 mV/s in all cases .....	61
Figure 27. Cyclic voltamogram of 10 mmol/ L HQ in 0.1 mol/L NaClO <sub>4</sub> ; at (a) nanohole PNA grafted GCE , (b) bare GCE, (c) PNA grafted GCE; Inset Cyclic voltamogram of nanohole PNA grafted GCE in supporting electrolyte (0.1 mol/L NaClO <sub>4</sub> ) at 50 mV/s in all cases.....	62
Figure 28. Cyclic voltamogram of 2 mmol/L DA in 0.1 mol/L sodium phosphate buffer (pH 7.5) at (a) nanohole PNA grafted GCE (b) at bare GCE; Inset Cyclic voltamogram of nanohole PNA grafted GCE in sodium phosphate buffer (pH 7.5) at 100 mV/s .....	65
Figure 29. Cyclic Voltamogram of 2 mmol/L DA in 0.1 sodium phosphate buffer (pH 7.5) at (a) nanohole PNA grafted GCE (b) bare GCE (c) nanohole Aph grafted GCE (D) nanohole PD grafted GCE at 100 mV/s in all cases. ....	66

Figure 30. Plot of oxidation peak current of 2 mmol/L DA vs pH at (i) bare GCE (ii) nanohole PNA grafted GCE in all cases scan rate 100 mV/s.....	68
Figure 31. Calibration curve of amperometric response of DA at (i) bare GCE (ii) nohole PNA grafted GCE.; inset (A) amperometric current vs time curve upon successive additions of 1 mol/L DA into a stirred system of 0.1 mol/L sodium phosphate buffer (B) amperometric response of phosphate buffer ( pH 7.5) at + 0.25 V. ....	70
Figure 32. Amperometric responses of 2 mmol/L DA and 200-fold excesses of interfering species at nanohole PNA grafted GCE at 0.25 V, inset amperometric response from interferent to DA.....	71

## List of Schemes

Schemes	pages
Scheme 1. Mechanism of formation of diazonium film on GCE; diazonium molecule is reduced at the electrode surface (A), forming a radical and N <sub>2</sub> is eliminated (B), the radical attacks the surface forming a covalent bond (C) .....	6
Scheme 2. Steps in modifying GCE .....	22

## List of Tables

<b>Contents</b>	<b>pages</b>
Table1 Effect of scan rate on oxidation peak current of $K_3Fe(CN)_6$ and HQ at the bare and nanohole 4-aminophenol grafted glassy carbon electrode.....	37
Table 2 Determination of AA in orange fruit using nanohole APh grafted GCE.....	44
Table 3 Determination of AA in vitamin C tablet using nanohole PD grafted GCE.....	44
Table 4 Effect of scan rate on oxidation peak current of $K_3Fe(CN)_6$ and HQ at the bare and nanohole p-Phenylenediamine grafted glassy carbon electrode. ....	50
Table 5 Determination of AA in orange fruit using nanohole PD grafted GCE.....	58
Table 6 Determination of AA in vitamin C tablet using nanohole PD grafted GCE.....	58
Table 7 Effect of scan rate on oxidation peak current of $Ru(NH_3)_6Cl_3$ and HQ at the bare and nanohole p-nitroaniline grafted glassy carbon electrode. ....	64
Table 8 Comparison of the Limit of Detection of the Fabricated Electrodes to Some Literatures.	72

## List of Abbreviation

CA	Chronoamperometry
CV	Cyclicvoltametry
GCE	Glassy carbon electrode
AuNPs	Gold nanoparticles
AuNPs/GCE	Gold nanoparticles deposited on glassy carbon electrode
ME	2-Mercaptoethanol
NEA	Nanoelectrode array
NEEs	Nanoelectrode ensembles
SAMs	Self-assembled monolayers
3D	Three dimensional diffusion

## **Acknowledgements**

I would like to express my deepest gratitude and respect to my advisors Dr. Tesfaye Refera and Mr. Shimeles Addisu for their endless support and guidance during the course of this work. Their communicative enthusiasm for chemistry and their encouragement have been greatly helped me and also I extend my genuine appreciation to Mr. Abiyot Kelecha for his suggestion when this thesis work was started. I would also like to acknowledge all of my teachers and my friends with whom I did the postgraduate study. My deepest gratitude goes to my parents and Sr. Firealem Chanalewu for their moral support and encouragement. Finally but not the last I would like to acknowledge Nole Kaba Woreda Administration Office and Chemistry Department, Jimma University, for their financial support and giving me the opportunity to work on this thesis.

## Abstract

The aim of this work was to increase sensitivity and selectivity in electroanalysis through surface nanostructuring. Electrode surface nanostructuring was done via electronucleation of gold nanoparticles (AuNPs) on Glassy carbon electrode (GCE). Gold nanoparticles deposited glassy carbon electrode was grafted with organic film using cyclic voltammetry. Three types of organic films were selected for surface modification; P-phenylenediamine (representing electropositive film), 4-aminophenol (representing neutral film) and p-nitroaniline (representing electronegative film). Nanoholes were produced by stripping deposited AuNPs and the fabricated electrodes were characterized using potassium hexacyanoferrate (negative redox probe), hydroquinone (neutral redox probe) and ruthenium hexamine chloride (positive redox probe). Sensitivity and selectivity of the modified electrodes were increased by analyzing electropositive analyte on electronegative film grafted nanostructured electrode and electronegative analyte on electropositive film grafted nanostructured electrode. Electroanalytical application of nanohole 4-aminophenol grafted GCE and nanohole P-phenylenediamine grafted GCE were studied for ascorbic acid (electronegative analyte) determination with their respective Limit of detection ( $LOD = 3\sigma/\text{slope}$ )  $0.626 \mu\text{ mol/L}$  and  $0.123 \mu\text{ mol/L}$  respectively. Electroanalytical application of nanohole p-nitroaniline grafted GCE was studied for detection of dopamine hydrochloride (electropositive analyte) with  $LOD 0.0611 \mu\text{mol/L}$ . Sensor response of AA and DA was not affected by possible interfering species and the three nanostructured electrodes showed good reproducibility and stability.



## **1 Introduction**

### **1.1 Electroanalysis**

Electroanalysis relates variation of electrical parameters like potential, current and charge to a chemical parameter (analyte concentration). Mostly science of electrochemistry is concerned with electron transfer between electrode and solution interface<sup>1</sup>. Therefore, structure of electrode-electrolyte interface where electrochemical reactions proceed is of decisive importance for electrode reactions. Electrochemical techniques have attracted great interest as its detection is fast, low in cost, with merits of low detection limit and high accuracy<sup>2</sup>. However, the major problem frequently encountered in the electrochemical detection is serious interferences caused by the substances with similar redox potentials at conventional electrodes and often suffer from a pronounced fouling effect, which results in poor selectivity and sensitivity<sup>3, 4</sup>. Thus, it is difficult to detect specifically one substance in the presence of others substances in real biological samples at conventional electrodes. So, electrode surfaces are modified in a quest to render an electrochemical function either not possible or difficult to achieve using conventional electrodes.

### **1.2 Chemically Modified Electrodes and Their Applications**

If one is able to control the physical and chemical properties of electrode-electrolyte interface, then an improvement in the properties of electrochemical reaction can be obtained. As a result electrode reaction can be affected by modification of the electrode surface via different modifiers. The modifiers can perform reaction parallel<sup>5</sup> to or in tandem<sup>6, 7</sup> with charge transfer and also can function as intermediate in redox-catalysis<sup>8</sup> or provide a stereo-selective environment<sup>9, 10</sup> for the electrode reactions.

Chemically modified electrode (CME) is electrode system whose electrochemical response substantially changes after modification of its surfaces<sup>11</sup>. The most distinguishing feature of chemically modified electrodes is their modification by a selected substance that is coated onto the electrode surface which endows the electrode certain desirable properties.

Glassy carbon electrode could be modified with a selected mono/multimolecular ionic or polymeric film<sup>12</sup>, the constitution of modifiers rationally designed to alter the electrode properties. In comparison to the bare electrodes, modified electrodes can provide selective interactions with the substrates, increased sensitivity and improved resistance to fouling<sup>13</sup>.

The use of nano materials for nanostructuring electrochemical sensors has aroused the interest of analysts<sup>14</sup>, because nanostructured materials improves selectivity and sensitivity of the sensor. As the size of electrode, decrease 3-dimensional (3D) diffusion of reactant toward the surface of the electrode increases and a higher number of chemisorbed electroactive molecules per area is observed for nanostructured electrodes than for bulk electrodes<sup>15</sup>. In this work nanostructuring of glassy carbon electrodes, characterization and studying of their application in electroanalysis is under taken.

## 1.3 Literature Review

### 1.3.1 Electrode Surface Modification

Increasing sensitivity and selectivity of electrode by modifying its surface has been one of the most active areas of research interest in electrochemistry<sup>16</sup>. Electrode modification is important part of the electrochemical studies that involves studies of the electrochemistry of the attached molecules and their specific applications in electro analytical determinations. Murray and co-workers<sup>17</sup> introduced the term chemically modified electrodes to describe electrodes that had foreign molecules deliberately immobilized on their surfaces. Since then researches on modification of electrodes have been expanding and these modifications are performed by adsorption modification, polymer film modification or covalent modification<sup>18</sup>. Covalent modification involves covalent immobilization of immobilized species on electrode surface. Carbon surface is found to be efficient for the covalent modifications due to its alterable functionalities; hence numerous investigations are made on attachments of the molecules of interest on carbon surfaces. Elliot and Murray<sup>19</sup> reported direct modification of electrode by azo linkage through the reaction of 2,4-dinitrophenylhydrazine with a surface of quinone group. Compounds like amino ( $\text{NH}_2$ ), aryl diazonium ( $\text{Ph-N}_2$ ) and arylacetate compounds are found to be more viable for covalent modification<sup>20-22</sup>. Modification procedure is simple, and covalent bond formed is strong, stable over both time and temperature<sup>20</sup>. Covalently modified electrodes have long-term stability and therefore various types of electrochemical sensors have been developed by electrochemical reduction of aryl diazonium salts<sup>23, 24</sup>.

Adsorption modification involves adsorption of modifiers from dilute solutions on electrodes<sup>25</sup>. Platinum and carbon have been the major electrode materials used for adsorption study<sup>26</sup>. Even though many interesting results have been obtained from surface modification of electrode by adsorption technique, these types of modifications do not usually stable as much as the covalently modified ones. Polymer film can modify electrodes by covalently bonding or by adsorption on the electrode surface<sup>27</sup> and this method forms multilayer on the surface of electrode as opposed to monolayers encountered for the other methods.

The electroactive polymers such as polypyrrole<sup>28</sup>, polyaniline<sup>29</sup> and nafion<sup>30</sup> are prepared by an electropolymerization procedure and used as modifier for the construction of the chemically modified electrodes<sup>31</sup>.

This method produces electrochemically very stable electrode surfaces and the electro activity of the electrode material is usually not destroyed by these films. These polymer films have also been observed to retain their own chemical behaviour, such as catalytic properties, when immobilized on the electrode surface.

A carbon paste electrode belongs to one type of carbon electrode promising electrochemical sensors of wide applicability<sup>32</sup>. Kuwana<sup>33</sup> has modified carbon paste electrode by introducing electrochemically active surface into the material. Baldwin<sup>34</sup> has described a simple method of direct mixing of a solid modifier to the paste which was the commencement of explosive research activity in this field. In contrast to the relatively complicated modifications of solid substrates, carbon pastes can be modified simply to obtain quantitatively new sensors with desired, often predefined, properties<sup>35</sup>; however, there is one aspect which makes them not very convenient for practical use and this is the necessity of refilling the carbon paste in experiments requiring a regular removal of the electrode surface layer.

### **1.3.2 Self Assembled Monolayer Strategies**

Assembling thin layers of molecular species on electrode surfaces enables the formation of chemically well defined surfaces and control of surface functionality so that selectivity of the sensor can increase. In surface modification, molecular species with specific functionality are attached to the surface, in a controlled manner, for example gold surfaces are very useful for electrochemical immunosensors as they are chemically inert and the oriented immobilization of antibodies onto gold is critical for a rational design of immunosensors<sup>31</sup>. The well established strategy of formation of a self-assembled monolayer for immobilization of biomolecules on gold surfaces are based on the strong attachment of thiol (SH) or disulfide (-S-S-) functional groups to Au (Fig. 1).

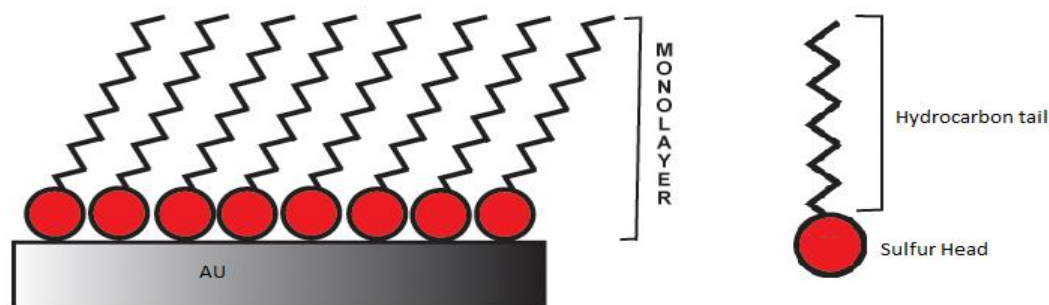


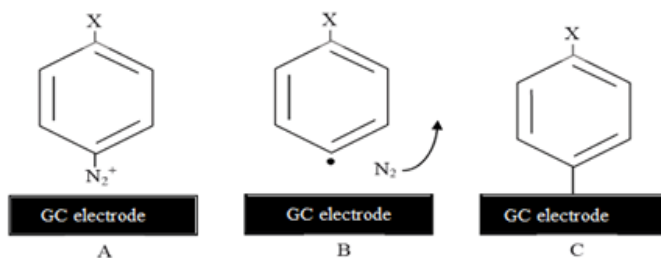
Figure 1. Self-assembled monolayers of thiols on gold

Alkanethiol self assembled monolayers (SAMs) are the most commonly used to covalently immobilize a biorecognition molecule (enzyme, antibody or nucleic acid sequence) onto the surface of the transducer since they offer the possibility of controlling orientation, distribution and spacing of the sensing element while reducing non-specific interactions<sup>36</sup>. The composite surface of GCE modified with gold nanoparticles offers the possibility of further site-selective modification, as GCE has no affinity towards thiol or disulfide groups in contrast to gold, on which thiol-based SAMs are readily formed. Thus, it is possible to protect or selectively functionalize spots on an overall conducting surface. Finot and coworkers<sup>36</sup> used a SAM of octadecanethiol to protect deposited Au nanocrystallites after the deposition step on GCE, then new gold nanoparticles electrodeposited from aqueous  $\text{KAuCl}_4$  solution without causing crystal growth because previously deposited gold nano particles already protected by an octadecanethiol film. The main limitation of self-assembly is the requirement of a specific functional group that will drive assembly onto the substrate of interest.

### 1.3.3 Grafting of Diazonium Salts on Glassy Carbon Electrode

Diazonium salts are a class of organic compounds prepared by treatment of aromatic amines with sodium nitrite in the presence of a mineral acid. Electrochemical reduction of aryl diazonium salts is one possible method for easy and efficient covalent modification of carbon electrode. The process of electrochemical reduction of in situ generated diazonium cation is favoured with the chemically irreversible loss of  $\text{N}_2$  from the diazonium ion moiety; this generates reactive aryl radicals near the electrode interface<sup>20</sup>.

Pinson and coworkers<sup>24</sup> investigated the modification of carbon surfaces based on electrochemical reduction of diazonium salts (4-nitrophenyl-1-diazoniumtetrafluoroborate in acetonitrile), which leads to a strong covalent binding of the 4-nitrophenyl group on the carbon surface rather than mere adsorption. One-electron reduction of aryl diazonium salt results in the formation of covalent bonding of aryl groups with carbon electrode surface. The binding of aryl groups to carbon electrodes is a two-step process. Initially diazonium salt is reduced at the electrode, with the elimination of N<sub>2</sub>. The second step is the reaction of the radicals with carbon surface to generate a covalent bond.



Scheme 1. Mechanism of formation of diazonium film on GC; diazonium molecule is reduced at the electrode surface (A), forming a radical and N<sub>2</sub> is eliminated (B), the radical attacks the surface forming a covalent bond (C)

### 1.3.3.1 Applications of Surface Modification via Electrochemical Reduction of Diazonium Salts

The irreversible interaction between diazonium derived aryl films and carbon has led to the application of this method to other materials such as metals<sup>37</sup> and semiconductors<sup>20</sup>. The advantages of diazonium reduction approach include a highly stable surface over time and over a wide potential window, ease of preparation, and the ability to synthesize diazonium salts with a wide range of functional groups<sup>24</sup>. In addition, the ability to create a diazonium-modified surface by the application of a potential bias allows the selective functionalization of closely spaced microelectrode surfaces. The use of carbon surfaces have dominated majority of the studies relating to the electro grafting of aryl diazonium salts<sup>20</sup>.

Detection of biological molecules using modified electrodes is more attractive strategy since electrochemical sensors combine the specificity and sensitivity for the needed biological or chemical response<sup>24</sup>.

### **1.3.4 Nanostructuring of Electrodes**

Metal and semiconductor nanoparticles can be immobilized on working electrode and modify its surface leading to specific and selective interactions with substrates<sup>13</sup>. Mono or multilayer arrays of conductive nanoparticles assembled on the electrode surfaces could be considered as assemblies of nanoelectrodes of controllable active areas<sup>38</sup>.

The preparation of hemispherical nanoelectrodes was introduced by Penner and coworkers<sup>39</sup> based on sequential electrochemical etching of microwires to a fine tip or cone and insulation of all but the very tip of the cone using a suitable insulator. Bard and co-workers<sup>40</sup> used a slightly different approach when preparing Pt nanotips. There has been much interest in the development of collections of nanoelectrodes which operate in parallel. If this collection is arranged in an ordered manner, with a controlled inter-electrode spacing, they are referred to as arrays; if the collection is not so ordered and there is not specific control over the inter-electrode spacing, then they are referred to as ensembles.

Nanoelectrode ensembles (NEEs) have been the subject of investigation by Martin and co-workers<sup>41,42</sup>. They have prepared disc arrays by the electrodeposition of metals within the micrometre and sub-micrometre-sized pores of polymeric porous membranes, referred to as the template synthesis method. A further approach to NEEs is to insulate a planar electrode and then open up holes in that insulation layer through underlying electrode. Baker and Crooks<sup>43</sup> have developed a technique based on etching of alkanethiol self-assembled monolayers (SAMs) from a gold surface, producing NEEs which can be characterized both by electrochemistry and scanning probe microscopy. The preparation procedure employs single crystal gold coated with a monolayer of underpotentially-deposited copper atoms. The thiolchemisorption takes place on top of this underpotentially-deposited copper layer; then nanoelectrodes are produced by electrochemically etching to enlarge native defects in the thiol SAM using cyanide solution.

Another SAM based approach suggested that active nanoelectrodes are redox species anchored at the ends of alkanethiol SAMs in which each redox-active molecule functions in the same way as an individual nanoelectrode<sup>44</sup>. Jeoung and co workers<sup>45</sup> used planar electrode coated with insulator which is used to block copolymer self-assembly to produce ordered arrays of pores on the electrode surface.

The pores mediated the transport of electroactive species to the underlying electrode surface thus enabling the system to perform as a nanoelectrode array (NEA). In this case, the pores are at regular distances from each other. Myrick and co-workers<sup>46, 47</sup> have reported two approaches for the preparation of recessed nanoelectrode arrays, based on the template synthesis method of Martin, producing NEEs rather than NEAs<sup>44, 45</sup>. Koehne and his coworkers<sup>48</sup> have reported fabrication of NEAs prepared from carbon nanotubes by combination with microlithography, it was possible to prepare NEAs with extremely low density of sites (i.e., of individual carbon nanotube). Such low density offers advantages to electroanalysis as it incorporates the enhanced mass transport to each carbon nanotube in the array while also having a lower charging current.

Metal and semiconductor nanoparticles have been widely used as electro-catalyst to achieve electrochemical detection of some organic molecules because of their high biocompatibility and catalytic activity<sup>49</sup>. Gold nanoparticles (AuNPs) are the most stable metal nanoparticles and have been widely studied<sup>50</sup>. There are various methods for the preparation of AuNPs, among them, the most convenient and popular method is chemical reduction in which metal ions are reduced by a reducing agent such as sodium borohydride, sodium citrate, hydrogen, and alcohol<sup>51</sup>. To avoid aggregation of metal colloids, a common strategy is to use a protecting agent such as thiols, surfactants, polymers, and dendrimers that can also control the particle size and introduce functionality to the particle surface<sup>15, 52</sup>.

Taking the advantage of a conducting carbon support known for not supporting alkanethiols SAM, metal nanoparticles can electrochemically deposited via the sequential deposition. In each deposition protection stage, the substrate is exposed to pure immobilising solution of an alkanethiol. The size and distribution of the domains in the SAM are assumed to follow the nanoparticles size and distribution during the nanostructuring stage<sup>15</sup>



### 1.3.5 Electrochemical Detection of Dopamine and Ascorbic Acid

In electrochemical methods chemically modified electrodes have been widely used as sensitive and selective for detection of trace amounts of biologically important compounds<sup>53, 54</sup>. Ascorbic acid is an important water-soluble substance present in many biological fluids, fruit juices, pharmaceuticals, soft drinks and vegetables. It is also added to foodstuffs as an antioxidant for stabilization of color and aroma, as well as for prolonging the life of commercial products<sup>55</sup>. Therefore, electrochemical determination of AA concentrations is considered essential for food quality and health care.

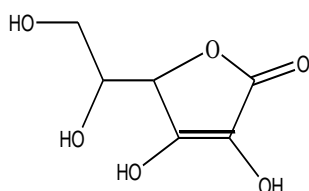


Figure 2. Molecular structure of ascorbic acid

Dopamine is one of the naturally occurring catecholamine present in a wide variety of animals, including both vertebrates and invertebrates. It is an important compound for message transfer in the mammalian central nervous system as well as in drug addiction and Parkinson's disease<sup>56, 57</sup>. Therefore, development of a simple and rapid method for the determination of DA with high selectivity and sensitivity is desirable for analytical applications.

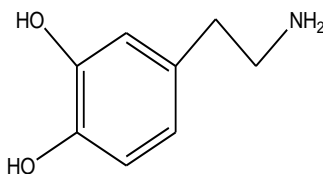


Figure 3. Molecular structure of dopamine

Even though electrochemical detection of AA and DA received much interest, the major problem frequently encountered is their redox reactions take place at very similar potentials and often suffer from a pronounced fouling effect at bare electrode<sup>58</sup>, which results in poor selectivity and reproducibility<sup>59, 60</sup>.

Different studies on determination AA and DA are based on different methods to separate either AA or DA by selecting specific potentials or using modified electrode<sup>61-62, 63</sup>. One of the most important properties of chemically modified electrodes is their ability to enhance sensitivity and selectivity in the electro analytical methods with respect to unmodified electrodes<sup>64</sup>.

AA exists in anionic form where as DA exists in cationic form at the physiological pH<sup>65, 66</sup>. Based on this property; different techniques have been developed to detect AA and DA<sup>67, 68</sup>. Modification of the working electrode with negatively charged substances like Nafion<sup>30</sup>, polypyrrole<sup>28</sup> and polyaniline<sup>29</sup> and integration of gold nanoparticles and novel functionalized matrix shows very promising applications in the fabrication of biosensors for sensitive and selective detection of dopamine and ascorbic acid.

Even though determination of AA and DA has been achieved using modified electrodes, adsorption of the analytes requires surface renewal after each experiment. Therefore, interest of analyst is still to develop simple, reliable, and efficient sensors for selective and effective detection of AA and DA simultaneously.

## **1.4 Theoretical Background**

### **1.4.1 Electrochemical Cell**

Electrochemical cell is fundamental apparatus for all electrochemical techniques and it is used for generating an electromotive force voltage and current from chemical reactions, or the reverse, inducing a chemical reaction by a flow of current. The current is resulted in electrochemical cell as the result of releasing and accepting of electrons at different ends of a conductor. Electrochemical cell involves electrolyte and electrodes. Working electrode is the terminal at which the electrochemical reaction occurs. Working and counter electrodes are immersed in the conducting electrolyte to complete the circuit. In order to apply a potential to the working electrode, a reference electrode of known potential is also required so that the potential of the working electrode can be measured. The reference electrode is connected to the potentiostat at a point with very high input impedance; this prevents current flowing through the reference electrode so that its potential maintained constant during the experiments.

### **1.4.2 Voltammetric Techniques**

Voltammetric techniques are electrochemical methods in which a time dependent potential is applied to an electrochemical cell, and current flowing through the cell is measured as a function of applied potential. Voltammetric technique makes use of a three-electrode system; working electrode, reference electrode and an auxiliary electrode. A plot of current which is directly proportional to the concentration of an electroactive species as a function of applied potential is called a voltammogram. Voltammogram provides both quantitative and qualitative information about the species involved in the oxidation or reduction reaction. Quantitative information is obtained by relating current to the concentration of analyte in the bulk solution and qualitative information is obtained from the voltammogram by extracting the standard-state potential for redox reaction. Concentration of the electroactive species can be quantitatively determined by measuring limiting current which is linear function of the concentration of electroactive species in the bulk solution. Half-potential serves as a characteristic of a particular species which undergoes reduction or oxidation process at the electrode surface in a given supporting electrolyte, and it is independent of the concentration of that species<sup>69</sup>.

The principle of this technique is a measurement of the diffusion controlled current flowing in an electrolysis cell. The earliest voltammetric technique was developed by Jaroslav Heyrovsky in the early 1920s and it is called Polarography<sup>70</sup>, since then different forms of voltammetric techniques like cyclic voltammetry and stripping voltammetry have been developed.

#### 1.4.2.1 Cyclic Voltammetry

Cyclic voltammetry (CV) is a potential-controlled reversal electrochemical experiment in which potential sweep is imposed on the working electrode and the current response is observed. Applied potential sweep backwards and forwards between two limits, the starting potential and the switching potentials. CV is the most widely used technique for acquiring qualitative information about electrochemical reactions<sup>71</sup>.

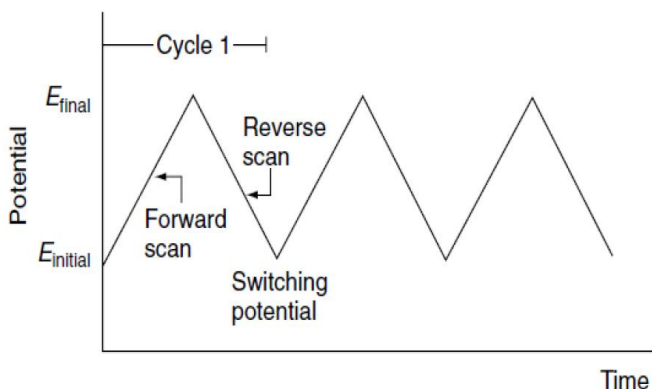


Figure 4. Potential-time stimulation signal of the cyclic voltammetry<sup>72</sup>

Analysis of the current response can give considerable information about the thermodynamics of redox processes, the kinetics of heterogeneous electron-transfer reaction and the coupled chemical reactions. CV in electrochemical study offers a rapid location of redox potentials of the electro active species. In this technique, the potential of the working electrode is increased linearly in an unstirred solution and the resulting cyclic voltammogram is observed. CV shows characteristics of an analyte by several important parameters such as peak currents and peak potentials that can be used in the analysis of the cyclic voltammetric response whether the reaction is reversible, irreversible or quasi-reversible<sup>71</sup>.

In reversible electrochemical reaction cathodic and anodic peak potentials are separated slightly. For redox process in reversible reaction, during the forward sweep the oxidized form is reduced, while on the reverse sweep the reduced form near the electrode is reoxidised. The peak currents are proportional to square root of the scan rate and the ratio of the peak current is equal to one. Formation of the diffusion layers near the electrode surface gives the characteristic peaks in the cyclic voltammogram. The peak current for a reversible couple (at 25°C), is given by Randles-Sevcik equation. This equation describes the effect of scan rate on the peak current in addition to the concentration and diffusional properties of the electroactive species.

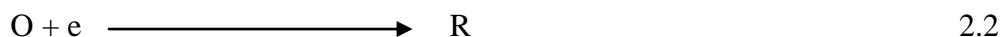
$$i_p = (2.69 \times 10^5) n^{3/2} A C D^{1/2} \nu^{1/2} \quad 2.1$$

Where  $i_p$ ,  $n$ ,  $A$ ,  $C$ ,  $D$ ,  $\nu$  are current maximum (in ampere), number of electrons, electrode area (in  $\text{m}^2$ ), concentration (in  $\text{mol m}^{-3}$ ), diffusion coefficient (in  $\text{m}^2 \text{s}^{-1}$ ) and the scan rate (in  $\text{V s}^{-1}$ ) respectively.

Irreversible electrochemical reaction is known by disappearance of the reverse peak and peak current is lower than that obtained by reversible reaction. Peak potential shifts with scan rate. In quasi-reversible electrochemical reaction, there is larger separation of cathodic and anodic peak potential compared to those of reversible systems.

#### 1.4.2.2 Chronoamperometry

Chronoamperometry (CA) is an electrochemical method in which a step potential is applied to working electrode and the current response is measured as a function of time. The current rises rapidly to a maximum value when the potential goes from its initial value; where there is no faradic reaction occurs, to its final value, where the electrochemical reaction of interest takes place at a diffusion-controlled rate<sup>73</sup>. Therefore, before determination of these potentials, redox potential must be known by running cyclic voltammogram of the analyte. For chemical reduction reaction of O to R (equation 2.2) with a formal potential  $E^0$ , the potential step applied to the working electrode should be sufficiently more negative than  $E^0$  such that reduction of O to R is complete at the surface of the electrode (i.e., concentration of O at the electrode surface become zero) and when this occurs, the current is diffusion-limited.



The analysis of CA data is based on the Cottrell equation, which defines the current-time dependence for linear diffusion control:

$$i = nFACD^{1/2}\pi^{-1/2}t^{-1/2} \quad 2.3$$

Where n, F, A, D, C are number of electrons transferred, Faraday's constant (96,500 C mol<sup>-1</sup>), electrode area (cm<sup>2</sup>), diffusion coefficient (cm<sup>2</sup> s<sup>-1</sup>) and concentration (mol m<sup>-3</sup>), respectively. Chronoamperometric measurement is used for determination of either D or A.

### 1.4.3 Nanotechnology and Nanoparticles

Nanotechnology is the study of manipulating matter on an atomic and molecular scale. Therefore, it deals with developing materials, devices, or other structures at nanometer scale in vast ranges of application, such as in medicine, electronics, chemistry and biomaterials etc<sup>74, 75</sup>. Nanoparticles are aggregates of atoms that are in the size range of 1 to 100 nm, though their sizes can extend up to several hundreds of nanometers. Particles size can be controlled by the types of synthesis methods including physical and chemical methods, then further characterized by various types of devices and applied to various fields. Generally there are two main approaches for making metallic films from nanoparticles: these are top-down and bottom-up techniques. Top-down technique is done via deposition of evaporated or sputtered metal from vacuum to a substrate or to a polymer matrix<sup>76</sup>. This approach is used to create smaller devices by using larger ones to direct their assembly. These methods include different technologies like that descended from conventional solid-state silicon methods for fabricating microprocessors and atomic layer deposition techniques.

Bottom-up technique is used to build up nanoparticles starting from atoms or molecules by applying suitable techniques. This approach is done via “soft” lithography stamping<sup>77</sup>, Self assembly of sterically protected nanoparticles<sup>78, 79</sup>, sol-gel coating<sup>80</sup>, or adsorption of nanoparticles onto oppositely charged substrates<sup>81</sup>.

#### 1.4.3.1 Properties and Importance of Nanoparticles

Mono or multilayer arrays of conductive nanoparticles assembled on the electrode surfaces may be considered as assemblies of nanoelectrodes of controllable active areas<sup>38</sup>.

Molecule and polymer-functionalized sensing surfaces of metal nanoparticles have been employed for developing all kinds of electrochemical sensors and nano-devices. The constructed sensors have special functions and could be applied to relate sensing or biosensing and bioelectronics research area, covering deoxyribonucleic acid hybridization, protein–protein interaction and small molecules determination, cell and microbe analysis, nanomedicine and so on<sup>64</sup>.

Metal and semiconductor nanoparticles, as sensing elements, could be immobilized and modify surface of working electrode by different kinds of methods including physical adsorption, chemical covalent bonding, electrodeposition, electropolymerization with redox polymers and so on<sup>64</sup>. The unique chemical and physical properties of nanoparticles<sup>82-84</sup> make them extremely suitable for designing new and improved sensing devices, especially electrochemical sensors and biosensors. Nanomaterials show different properties from bulk materials due to size effect: atoms at the surface have lower coordination numbers and are therefore less stable than the bulk atoms. Smaller the particle size, the larger the fraction of atoms at the surface, and thus the more reactive is the surface, which makes nanosized materials of immense interest as substrates for biosensor applications<sup>15</sup>.

#### **1.4.4 Deposition of Metal Nanoparticles**

Electrochemical deposition is a rapid and easy procedure for production of nanoparticles on conducting surfaces. It can be occurred by applying potential difference at the electrode-electrolyte interface which results in electron transfer between electrode and ionic species in the electrolyte and subsequent deposition of atoms of this species onto the electrode surface. The current transferred during the electrochemical deposition of atoms is related to the charge (Q) passed in the process (equation 2.4).

$$Q = it \tag{2.4}$$

Where *i* is current in ampere and *t* is time in second.

According to Faradays law, charge consumed during electrochemical deposition can also be related to the mass of species (equation 2.5).

$$Q = nFN$$

2.5

Where N, n, F are number of moles of depositing species reacted, number of electrons involved in redox reaction and Faraday's constant (96,487 C), respectively.

#### 1.4.5 Microelectrodes and Nanoelectrodes

Microelectrodes are electrodes with critical dimensions smaller than at least 25  $\mu\text{m}$ ; where critical dimension is dimension which controls the electrochemical response. Any submicrometre electrode can be viewed as a nanoelectrode; where nanoelectrode is electrode with a critical dimension in the nanometre range. Generally, ultra microelectrode can be viewed as any electrode in which its magnitude is smaller than the diffusion layer, yielding an electrode with a critical dimension (e.g., radius) of the order of 25  $\mu\text{m}$ . When the electrode's critical dimension is further decreased to the same order as the thickness of the molecular size, the experimental behaviour starts to deviate from extrapolations of behaviour at larger electrodes<sup>85</sup>.

The great advantage of using ultra microelectrodes is the benefit obtained from the enhanced mass transport<sup>86, 87</sup>. As electrodes decrease in size, 3D becomes dominant and results in faster mass transport. This high rate of mass transport at small electrodes enables measurement of kinetics by steady-state experiments techniques. When electrode size is decreased from micrometre to nanometre scale, study of faster electrochemical reaction could be possible; because electron transfer process is less likely to be limited by the mass transport of reactant to the electrode surface at very high rates of mass transport<sup>39, 88</sup>. Due to the extreme smallness of the active regions of nanoelectrodes, it is possible to pack many nanoelectrodes onto a given footprint of a sensor device. The smaller the active electrode surface, the more of these materials can be constructed within the allotted area of a sensor system or other measurement device. The catalytic properties of metal nanoparticles could decrease over potential of some important reactions in electrochemical analysis and even provide electrochemical reversibility for redox reactions which are irreversible at traditional bulk electrodes<sup>89</sup>, sometimes, could further enhance the electrochemical responses greatly.



### 1.4.6 Geometry of Nanoelectrodes

Electrochemical study of nanoelectrodes and nanoelectrode arrays is important from a characterization as well as possible application perspective.

It was not possible to see the tips of such electrodes using scanning electron microscopy thus the electrochemical response was used to infer the dimensions of the surface. To solve this problem it is possible to totally dependent on the electrochemical signal by relating it to the electrode dimensions, typically the radius. Nanoelectrode critical parameter, radius of the disc, for example, is extracted by applying a suitable model for the steady-state current. Figure 5 illustrates possible diffusion modes and corresponding steady-state current equations for hemisphere, inlaid disc and recessed disc electrodes<sup>39, 88, 90</sup>.

Based on the fabrication procedures of individual nanoelectrodes, the nanoelectrodes which are prepared by the etching/partial insulation approach produce nanocones and have been approximated by the hemisphere model. The recessed disc model has been employed to characterise nanoelectrodes deliberately prepared with a wax sheath surrounding and extending beyond the electrode surface, i.e., recessed nanoelectrodes<sup>91</sup>.

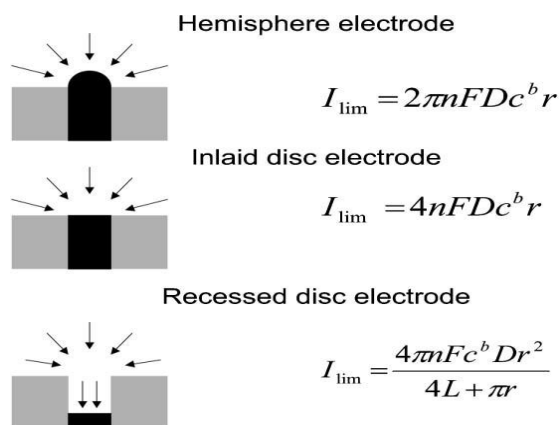


Figure 5. Nanoelectrode geometries: hemispherical electrode, inlaid disc electrode and recessed disc electrode; diffusion modes and the equations for the corresponding steady-state currents. Here,  $n$ -number of electrons involved in the redox process,  $F$ -faraday's constant,  $D$ -diffusion constant ( $\text{cm}^2\text{s}^{-1}$ )  $r$ -nanoelectrode radius (m),  $L$ -recessed height (m)

### 1.4.7 Mass Transport to Nanoelectrodes

The most important factor determining behavior of an electrode is the mass transport in solution in the vicinity of the electrode. Mass transport is the movement of material from one location to another in the solution<sup>92</sup>. Three modes of mass transport considered in electrochemical systems are diffusion, convection, and migration. Diffusion is a microscopic and random movement of species in a concentration gradient from region of high to low concentration. When considering an uncomplicated charge-transfer reaction, voltammetric current signal is proportional to the flux of the electroactive substance  $C(x, y, z)$  toward the solution–electrode interface described by Fick’s first law which is mathematically described as:

$$J = \frac{-D\partial C(x,t)}{\partial x} \quad 3.3$$

Where  $J$  is flux of material, i.e., moles passing a  $1 \text{ m}^2$  plane at point  $x$  and time  $t$  ( $\text{mol}/\text{m}^2/\text{sec}$ ),  $D$ , is diffusion coefficient ( $\text{m}^2/\text{sec}$ ),  $C$  is concentration,  $t$  is time (sec) from when power is turned on and  $x$  is distance from electrode surface (cm). Fick’s second law describes time-dependent changes in the concentration of the substance which is mathematically described as:

$$\frac{\partial C}{\partial t} = D \frac{\partial^2 C}{\partial x^2} \quad 3.4$$

Convection is the movement of species due to mechanical forces. There are two forms of convection; natural and forced. Natural convection is a macroscopic movement of layers of fluid due to temperature, pressure, density gradients and forced convection occurs when the movement of particle is due to external forces<sup>93</sup>.

$$J_{convection} = C.V \quad 3.5$$

Where  $J$  is flux of material i.e., moles passing a  $1 \text{ cm}^2$  plane,  $C$  is concentration (in  $\text{mol m}^{-3}$ ) and  $V$  is fluid velocity (in  $\text{ms}^{-1}$ )

Mass transport due to convection can be eliminated using quiescent solution, but it is impossible to completely eliminate natural convection. Migration is the movement of charged species due to a potential gradient. Migration could totally be eliminated by the addition of a fully dissociated electrolyte, which acts as the ionic charge carrier.

## 1.5 Statement of the Problem

Nanoparticles attract substantial interest because they exhibit unique optical, electrical, thermal and catalytic properties. It is possible to change their size and shape and manipulate them with different materials to prepare a broad range of nanostructures with different physical and chemical properties. Metal and semiconductor nanoparticles as sensing elements could be immobilized on working electrode surface by kinds of methods including physical adsorption, chemical covalent bonding, electrodeposition, electropolymerization with redox polymers and so on. The unique chemical and physical properties of nanoparticles make them extremely suitable for designing new and improved sensing devices, especially electrochemical sensors and biosensors. Thus, the present work can answer the following questions:

- ✚ What electrode modification using nanotechnology can be devised to improve sensitivity of electro analytical determinations?
- ✚ What nanotechnology solution can be exploited for improving selectivity of electrodes?

## 1.6 Hypothesis

- ✓ Nanoelectrodes have advantage compared to bulky electrodes to improve sensitivity of electro analytical determinations by increasing mass transport of analyte towards electrode surface.
- ✓ Selectivity of electro analytical determinations can be improved by controlling electrode surface charge.

## **1.7 Objectives of the Study**

### **1.7.1 General Objective**

To enhance sensitivity and improve selectivity of electro analytical sensors by fabricating nanoelectrode assemblies.

### **1.7.2 Specific Objectives**

- ✓ To electroplate gold nanoparticles on glassy carbon electrode and characterize the modified electrode by electrochemical method.
- ✓ To electro graft p-aminophenol, p-phenylenediamine and p-nitroaniline diazonium salts on the surface of glassy carbon electrode and characterize the film formed electrochemically.
- ✓ To fabricate randomly nanoarrayed electrodes by combining Procedures for electroplating of gold nanoparticles and p-aminophenol, p-phenylenediamine and p-nitroaniline diazonium salts electro-grafting.
- ✓ To characterize the fabricated surface by comparing electrochemical response of redox probes like  $K_3[Fe(CN)_6]$ ,  $Ru(NH_3)_6Cl_3$  and hydroquinone at bare glassy carbon electrode,.
- ✓ To apply the fabricated nanohole electrodes for electroanalysis of some selected model analytes.

## **2 Materials and Methods**

### **2.1 Electrochemical Measurement**

All electrochemical measurements were performed with Epsilon electrochemical analyzer (Bioanalytical System Inc. USA model) and a conventional three-electrode system, comprising a GCE working electrode (3 mm diameter, BAS Model ), a platinum wire as an auxiliary electrode and Ag/AgCl 3 mol/L NaCl electrode as reference. All potentials were reported versus the Ag/AgCl reference electrode at room temperature.

## 2.2 Chemicals and Reagents

p-Phenylenediamine [ $C_6H_8N_2$ , 100 %, Aldrich], 4-aminophenol [ $C_6H_7NO$ ,  $\geq 99\%$ , Aldrich], para-nitro aniline [ $C_6H_6N_2O_2$ , 99%, Kiran], sodium nitrite [ $NaNO_2$ , 96%, Wardle], potassium nitrate [ $KNO_3$ , 99%, Nice], potassiumtetrachloroaurate [ $KAuCl_4$ , 99.99%, Aldrich], potassium hexacyanoferrate [ $K_3Fe(CN)_6$ , 99%, BDH Laboratory], 2-mercaptoethanol [ $HSCH_2CH_2OH$ , 100 % Aldrich], hydrochloric acid, [ $HCl$ , 37%, Riedel-De Haen], sulphuric acid, [ $H_2SO_4$ , 98%, Merck], hydroquinone [ $C_6H_6O_2$ , 99%, Kiran], hexamine ruthenium- chloride (III) [ $Ru(NH_3)_6Cl_3$ , 98%, Aldrich], potassium iodide [ $KI$ , 99%, Nice], iodine resublimized [ $I_2$ , 99.5%, Nice], potassium chloride [ $KCl$ , 99%, Finkem], sodium citrate [ $Na_3C_6H_5O_7 \cdot 2H_2O$ , 99%, Finkem], dopaminehydrochloride injection [Chandra Bhagat Pharma], ascorbic acid 500mg [ $C_6H_8O_6$ , Ethiopian pharmaceuticals], sodium acetate [ $C_2H_3NaO_2 \cdot 3H_2O$ , 99.8%, Chem. Rein], glacial acetic acid [ $CH_3COOH$ , 100%, BDHL Laboratory], citric acid [ $C_6H_8O_7$ , 99%, Wardle], potassium hydrogen phosphate [ $K_2HPO_4$ , 98 %, Finkem], potassium dihydrogen phosphate [ $KH_2PO_4$ , 99%, Nice] were of analytical grade reagents and used as received. Distilled water was used to prepare all solutions.

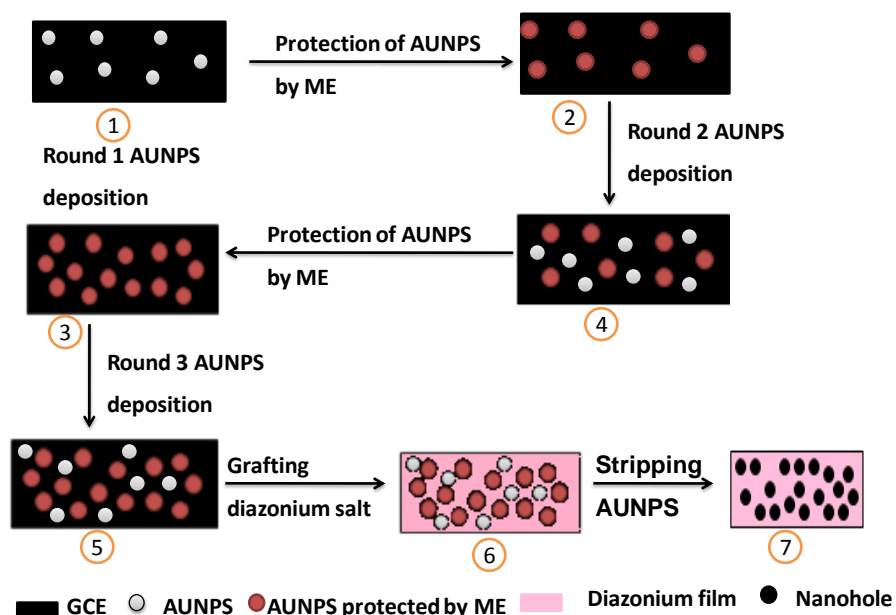
## 2.3 Experimental Procedures

### 2.3.1 Electrode Pretreatment

Prior to electrode modification, bare glassy carbon electrode was polished with a polishing paper and then further polished to a mirror finishing with alumina slurries and rinsed thoroughly with distilled water.

### 2.3.2 Fabrication of Randomly Nanoarrayed Electrodes

Fabrication of randomly nanoarrayed electrode was undertaken in seven steps (scheme 2). These steps are; (i) Electrodeposition of AuNPs<sup>15, 36</sup> (step 1 to 5), (ii) Grafting of diazonium films (step 6) and (iii) Stripping of the deposited AuNPs (step 7). For all modifications these steps are the same except grafting stage (step 6) where the three different organic films with different property were used at different modification time.



Scheme 2. Steps in modifying GC

#### (i) Electrodeposition of Gold Nanoparticles

Gold nanoparticles were electrodeposited on GCE following the literature<sup>15</sup> procedure. This was done first by adding 10  $\mu\text{L}$  of 0.5 mol/L  $\text{KAuCl}_4$  in 5 mL of 0.5 mol/L  $\text{H}_2\text{SO}_4$  in an electrochemical cell. Then chronoamperometry (CA) was run with general parameters of initial potential of 0 V stepped to 1.1 V for a 5 s at scan rate of 50 mV/s. To prevent crystal growth of AuNPs, the modified GCE was kept upside down in 50  $\mu\text{L}$  of 2 mmol/L 2-mercaptoethanol (ME) capping agent in a micropipette tip for 2 hour at room temperature after each deposition steps.

## **(ii) Grafting of Diazonium Films**

This step is the only step that makes the three nanostructured electrode modification type different. Three types of diazonium salts with different electrochemical properties were used to control surface charge of nanostructured electrodes. These were (A) 4-aminophenol (designed to represent electroneutral film), (B) p-Phenylenediamine (designed to represent electropositive film), and (C) p-nitroaniline (designed to represent electronegative film). Grafting of each diazonium films on nanostructured electrodes, their electrochemical characterization and their application in electroanalysis was studied one by one.

### **A. Grafting of 4-Aminophenol Film**

AuNPs modified GCE was grafted with in situ prepared 4-aminophenol diazonium cation based on the literature<sup>49</sup> procedure. Briefly, 30 mL of 3 mmol/L 4-aminophenol in 0.5 mol/L HCl and 30 mL of 0.1 mol/L sodium nitrite were kept separately in ice jacketed beaker for 1 hour. Then, 400  $\mu$ L of 0.1 mol/L NaNO<sub>2</sub> was added to 20 mL of 3 mmol/L 4-aminophenol (Aph) in 0.5 mol/L HCl under stirring at room temperature and CV was used to graft APh film on AuNPs nucleated GC from potential window of 0.6 V to -0.2 V at a scan rate of 0.1 V/s for 3 cycles.

### **B. Grafting of p-Phenylenediamine Film**

The AuNPs modified GCE was grafted with the in situ prepared p-Phenylenediamine (PD) diazonium cation based on the literature information<sup>49, 94</sup>. Briefly, 5 mL solution of 3 mmol/L PD in 0.5 mol/L HCl and 5 mL of 3 mmol/L sodium nitrite in 0.5 mol/L HCl were kept separately in ice jacketed beaker for 1 hour. Then, 2 mL of 3 mmol/L NaNO<sub>2</sub> was added to 2 mL of 3 mmol/L PD under stirring at room temperature and CV was used to graft nitrophenyl film on AuNPs nucleated GC from potential window of 0.6 V to -0.2 V at a scan rate of 0.1 V/s for 3 cycles.

### **C. Grafting of P-nitroaniline Film**

The AuNPs modified GCE was grafted with in situ prepared nitrophenyl diazonium cation according to the literature procedure<sup>95</sup>. Firstly, 100 mL of 3 mmol/L p-nitroaniline (PNA) in 0.5 mol/L HCl and 10 mL of 0.1 mol/L NaNO<sub>2</sub> were kept separately in an ice jacketed beaker for 1 hour. Then 400 µL of 0.1 mol/L NaNO<sub>2</sub> was added to 20 mL of 3 mmol/L PNA in 0.5 mol/L HCl under stirring at room temperature and CV was used to graft nitrophenyl film on AuNPs nucleated GC from potential window of 0.6 V to -0.2 V at a scan rate of 0.1 V/s for 3 cycles.

#### **(iii) Stripping of Deposited Gold Nanoparticles**

For all modification types, nanoholes were produced by stripping the deposited AuNPs in 0.1 mol/L KCl using CV in a potential range of 0 mV to 1400 mV for three cycles.

### **2.3.3 Electrochemical Characterization of Randomly Nanoarrayed Electrodes**

The prepared electrodes were electrochemically characterized by CV using hydroquinone (neutral redox probe), Ru(NH<sub>3</sub>)<sub>6</sub>Cl<sub>3</sub> (positive redox probe) and K<sub>3</sub>Fe(CN)<sub>6</sub> (negative redox probe). The signal of these probes at nanohole electrodes were compared to signals at bare GCE, both at low and high scan rates.

### **2.3.4 Preparation of Ascorbic Acid Solutions**

Stock solutions of 2 mmol/L ascorbic acid was prepared in 0.1 mol/L acetate buffer solutions (pH 5) and other intermediate solutions of ascorbic acid were prepared by appropriate dilution of the stock solution in acetate buffer solution (pH 5). Amperometric method was used for detection of the samples. For calibration plots of the samples, average values of three measurements were taken for each concentration.

### **2.3.5 Preparation of Dopamine Solution**

2 mmol/L DA was prepared in 0.1 mol/L Phosphate buffer solution (pH 7.5) and other intermediate solutions of dopamine were prepared by appropriate dilution of the stock solutions in phosphate buffer solution (pH 7.5). Amperometric method was used for detection of the samples. For calibration plots of the samples, average values of three measurements were taken for each concentration.



### **2.3.6 Preparation of Solutions of Interferents**

For interference study of ascorbic acid, solution of 0.4 mol/L caffeine, 0.4 mol/L glucose, 0.4 mol/L sucrose, 0.4 mol/L starch, 0.4 mol/L citric acid, 0.4 mol/L oxalic acid, 0.4 mol/L tartaric acid and 0.2 mol/L uric acid were prepared in 0.1 mol/L acetate buffer solution (pH 5). Interference study was done amperometrically at nanohole Aph grafted GCE and nanohole PD grafted GCE at potentials of 0.25 V and 0.237 V, respectively.

For interference study of dopamine solution of 0.2 mol/L ascorbic acid (AA), 0.2 mol/L uric acid (UA), 0.2 mol/L citric acid (CA), 0.2 mol/L glucose (GLU) and 0.2 mol/L tartaric acid (TA) were prepared in 0.1 mol/L phosphate buffer (pH 7.5). Interference study was done amperometrically at 0.25 V at nanohole PNA grafted GCE.

### **2.3.7 Analysis of Real Samples**

Orange fruit was obtained from local market. Fresh juice of orange was obtained by squeezing orange fruit into a glass beaker then the juice was filtered through filter paper to remove the fibre and pulp. Then, 1 mL juice was diluted with 5 mL of 0.1 mol/L sodium acetate buffer (pH 5). Chronoamperometric analysis was done three times at 0.25 V at nanohole Aph grafted GC and at 0.237 V at nanohole PD grafted GC and average results of the three measurements were taken. Concentration of ascorbic acid was determined through standard addition method.

For determination of AA in vitamin C tablet solution of vitamin C tablet was prepared according to literature procedure<sup>96</sup>. Briefly one tablet was crushed with a mortar and pestle and the powder was dissolved in 20 mL of distilled water and then 10 mL of 1 mol/L H<sub>2</sub>SO<sub>4</sub> was added then, 9.3 mL of solution was taken and diluted with 20 mL sodium acetate buffer. For amperometric determination of AA in vitamin C tablet, 1 mL of the solution was taken and added to electrochemical cell that contains 5 mL of sodium acetate buffer. CA analysis was done three times at nanohole Aph grafted GCE at 0.25 V and at nanohole PD at 0.237 V grafted GCE and average results were taken.

The reliability of the amperometric determination of ascorbic acid in orange fruit and vitamin C tablet was verified using an iodimetric titration<sup>97</sup>. For this purpose, 10 mL of filtered fruit juice pipetted into a 250 mL erlenmeyer flask and then 100 mL of distilled water and 10 mL of starch solution were added, and then the content of the solution was titrated with 0.05 mol/L standardized iodine solution. Iodine solution was standardized by 0.1 mol/L standard sodium thiosalphate. For titrimetric determination of AA in vitamin C tablet, solution of vitamin C tablet was taken into 250 mL flask, and then 1mL portion of starch solution was added. Then the solution was titrated with the 0.05 mol/L iodine solution. The endpoint of titration was identified as the first distinct trace of a dark blue-black colour due to the starch-iodine complex. Titration was repeated three times and average result was taken in each case.

### 3 Results and Discussion

#### 3.1 Electrodeposition of Gold Nanoparticles

Gold nanoparticles were deposited from a solution of 0.1 mmol/L  $\text{KAuCl}_4$  in 0.5 mol/L  $\text{H}_2\text{SO}_4$ . Cyclic voltammetric experiment was made using GCE in the gold solution (Figure 6) to select the potential for deposition of gold on a GCE surface. The reduction peak current around 0.68 V shows deposition of gold on the surface of the electrode. The oxidation peak current observed around 1.2 V is due to gold oxide layer formation on the surface of GCE which was reduced in the reverse scan around 0.95V. Deposition of gold on GCE was confirmed by running of cyclic voltamogram of the electrode on which gold was deposited in the supporting electrolyte that shows sharp cathodic peak at 0.953 V which corresponding to reduction of gold oxide layer formed on the surface the electrode (Figure 6 inset) and Similar result was reported by Tesfaye and coworkers<sup>55</sup>. After cyclic voltammetry study of  $\text{KAuCl}_4$  sequential deposition of AuNPs was done from the solution of 0.1 mmol/L  $\text{KAuCl}_4$  using chronoamperometry<sup>55</sup>. To increase the number of nanoparticles (prevent secondary nucleation) ME self assembled was used in sequential deposition as it has also been described in experimental part.

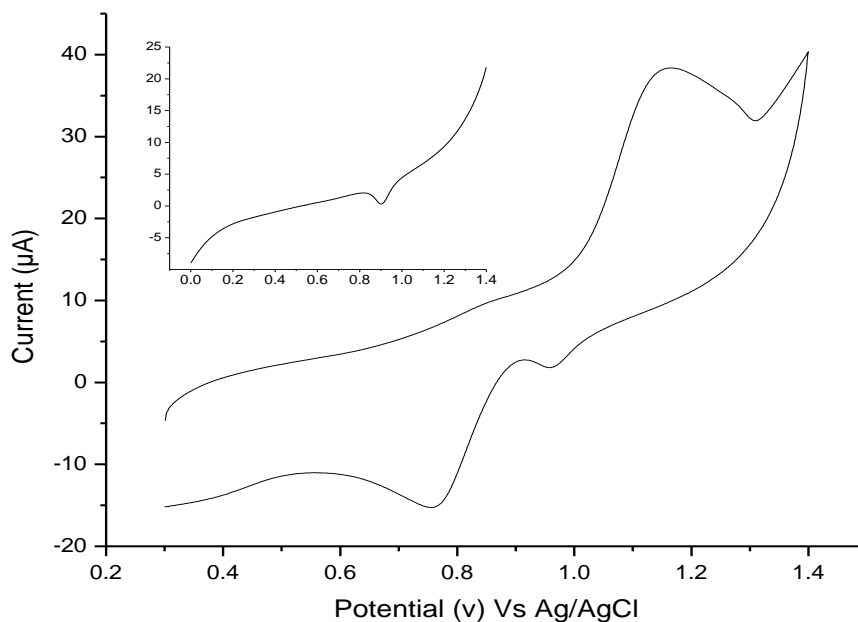


Figure 6. Cyclic voltammogram of 0.1 mmol/L  $\text{KAuCl}_4$  in 0.5 mol/L  $\text{H}_2\text{SO}_4$ ; Inset reduction of a gold oxide layer formed at a scan rate of 50 mV/s

### **3.2 Grafting Diazonium Salts on Glassy Carbon Electrode**

Grafting of each diazonium films on GCE were studied on bare electrode before nanostructuring. Redox probe voltammetry is a useful technique for confirming the formation of films on the electrode surface<sup>98, 99</sup>. After sequential deposition of AuNPs, grafting of diazonium film on AuNPs deposited GCE was undertaken. The three diazonium films primarily used in this study were grafted on bare GCE and AuNPs deposited GCE separately. Each diazonium film modified electrodes characterized electrochemically and applications of the nanostructured electrodes were studied one by one.

### 3.2.1 Grafting of 4-Aminophenol Film

Figure 7 shows grafting of 4-aminophenol on bare and AuNPS deposited GCE and nanohole Aph grafted GCE formation. Aminophenol reduced around 0.45 V both at bare GC and AUNPS AuNPs deposited GCE. Oxidation peak current observed in the first cycle was attributed to oxidation of amine to its analogous cation radical which form chemically stable covalent linkage between phenyl ring and GCE; the disappeared of oxidation peak in subsequent cycle is due to insulation effect of grafted the surface film.

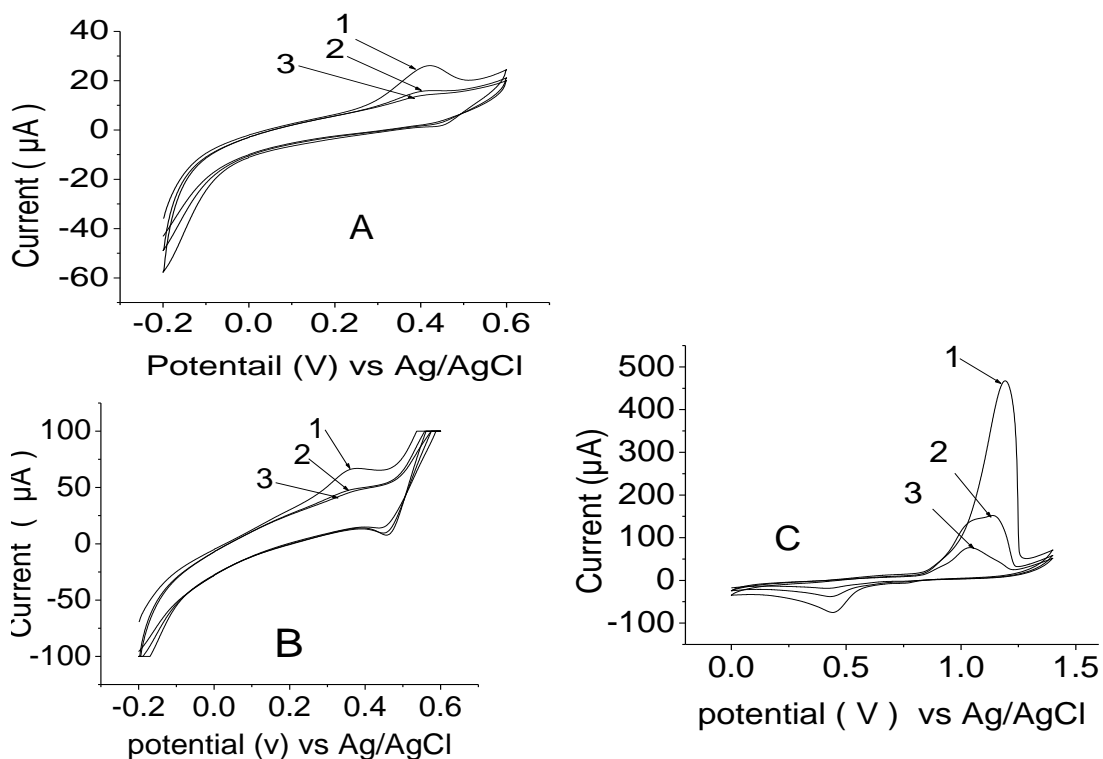


Figure 7. Cyclic voltammogram of grafting of 3 mmol/L 4-aminophenol at (A) bare GCE and (B) AuNPs deposited GCE in 0.5 mol/L HCl ( $v=100$  mV/s) (C) Cyclic voltammogram of AuNPs nucleated 4-aminophenol modified GCE in 0.1 mol/L KCl ( $v = 100$  mV/s) for 3 cycles (1, 2, 3 representing first cycle, second cycle and third cycle, respectively)

Formation of 4-aminophenol film on GCE was further proved by voltammetric studies of  $\text{Ru}(\text{NH}_3)_6\text{Cl}_3$ ,  $\text{K}_3\text{Fe}(\text{CN})_6$  and HQ solutions where suppression for redox peak was observed with respect to  $\text{Ru}(\text{NH}_3)_6\text{Cl}_3$  and HQ, redox peak of  $\text{K}_3\text{Fe}(\text{CN})_6$  probe was enhancement at 4-aminophenol grafted GCE relative to bare GCE. After modifying GCE with AuNPs and grafting 4-aminophenol film, the next step was producing nanoholes. This was achieved by stripping the nucleated AuNPs in 0.1 mol/L KCl using CV from 0 V to 1.4 V with six cyclic scan. As can be shown in Figure 7 C, anodic peak current observed around 0.97 V is due to oxidation of AuNPs. The magnitude of anodic peak current decreased in subsequent cycles indicating complete removal of the deposited AuNPs. The production of nanohole 4-aminophenol grafted glassy carbon electrode (nanohole Aph grafted GCE) was further proved by its enhancement of redox peak current of  $\text{K}_3\text{Fe}(\text{CN})_6$  and HQ, and suppression of redox peak current of  $\text{Ru}(\text{NH}_3)_6\text{Cl}_3$ .

### 3.2.2 Grafting of P-Phenylenediamine Film

P-phenylenediamine grafted on bare and AuNPs deposited GCE and characterized electrochemically. As can be seen from Figure 8 cyclic voltamogram of PD grafting film on bare GCE and AuNPs deposited GCE and formation nanohole PD grafted GCE shown one by one. Broad, irreversible anodic peak observed in the first cycle at  $-0.077$  V at bare GCE and at  $0.04$  V AUPS deposited GCE and no cathodic peak observed on the reverse scan indicate species obtained after the first electron transfer undergoes a chemical reaction. During this process p-phenylenediamine oxidized electrochemically and turns into cation radical; then, these cation radicals form C-C covalent bonds with electrode surface. The gradual decrease of oxidation peak current is due to insulation effect of grafted surface film. Furthermore, formation of PD film on GCE was further proofed by cyclic voltammetry of  $\text{Ru}(\text{NH}_3)_6\text{Cl}_3$ ,  $\text{K}_3\text{Fe}(\text{CN})_6$  and HQ. Redox peak of  $\text{K}_3\text{Fe}(\text{CN})_6$  and HQ enhanced and redox peak of  $\text{Ru}(\text{NH}_3)_6\text{Cl}_3$  suppressed relative to at bare GCE.

After modifying GCE with AuNPs and grafting p-phenylenediamine film the next step was producing nanoholes. This was achieved by stripping the nucleated AuNPs in 0.1 mol/L KCl using CV from 0 V to 1.4 V with six cyclic scans at a scan rate of 100 mV/s. Anodic peak observed around 0.97 V is due to formation of AuNPs oxide and its magnitude decreased in subsequent cycles indicating complete removal of the deposited AuNPs (Figure 8 C).

The production of nanohole p-phenylenediamine grafted glassy carbon electrode (nanohole PD grafted GCE) was further proved by enhancement of redox current peak of  $K_3Fe(CN)_6$  and HQ, and suppression of redox current peak of  $R(NH_3)_6Cl_3$  redox probes.

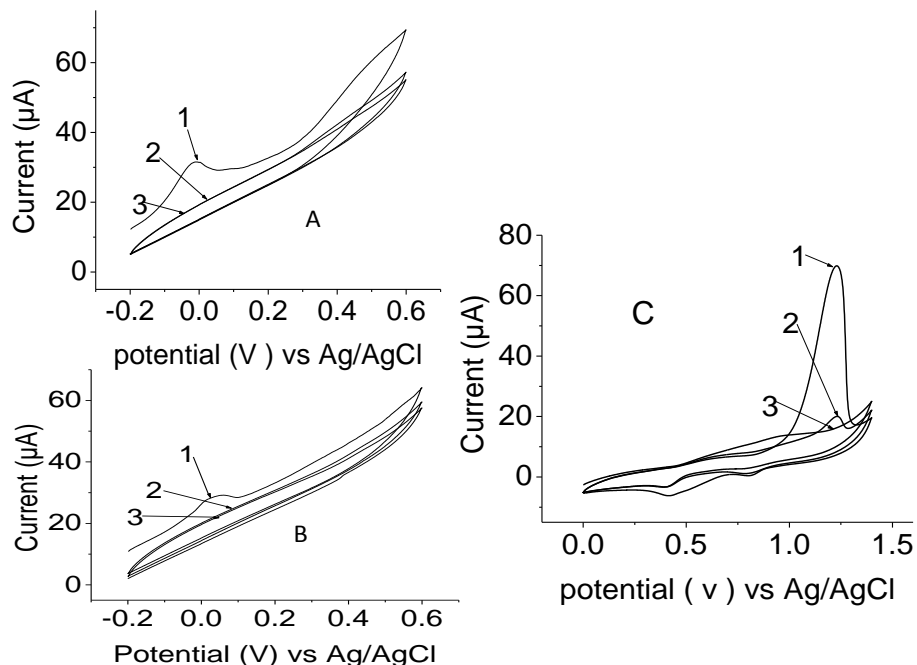


Figure 8. Cyclic voltammogram of grafting of 3 mmol/L p-phenylenediamine in 0.5 mol/L HCl at (A) bare GCE and (B) AuNPs deposited GCE in 0.1 mol/L KCl; (C) Cyclic voltammogram of AuNPs nucleated p-phenylenediamine modified GCE for 3 cycles (1, 2 and 3 representing first cycle, second cycle and third cycle respectively) in all cases scan rate 100 mV/s

### 3.2.3 Grafting p-Nitroaniline Film

P-nitroaniline film grafted on bare glassy GCE and AUNPS deposited GCE and characterized electrochemically. As can be seen from Figure 10 redox peak of the p-nitroaniline at bare GCE as well at AuNPs deposited GCE electrode, decrease in the subsequent sweeps indicate monolayer coverage of p-nitroaniline films on the electrodes surface<sup>100</sup>. Formation of PNA film on GCE was further proved by its insulation ability of redox current peak of  $K_3Fe(CN)_6$  and HQ probes and enhancement of redox current peak of  $Ru(NH_3)_6Cl_3$ .

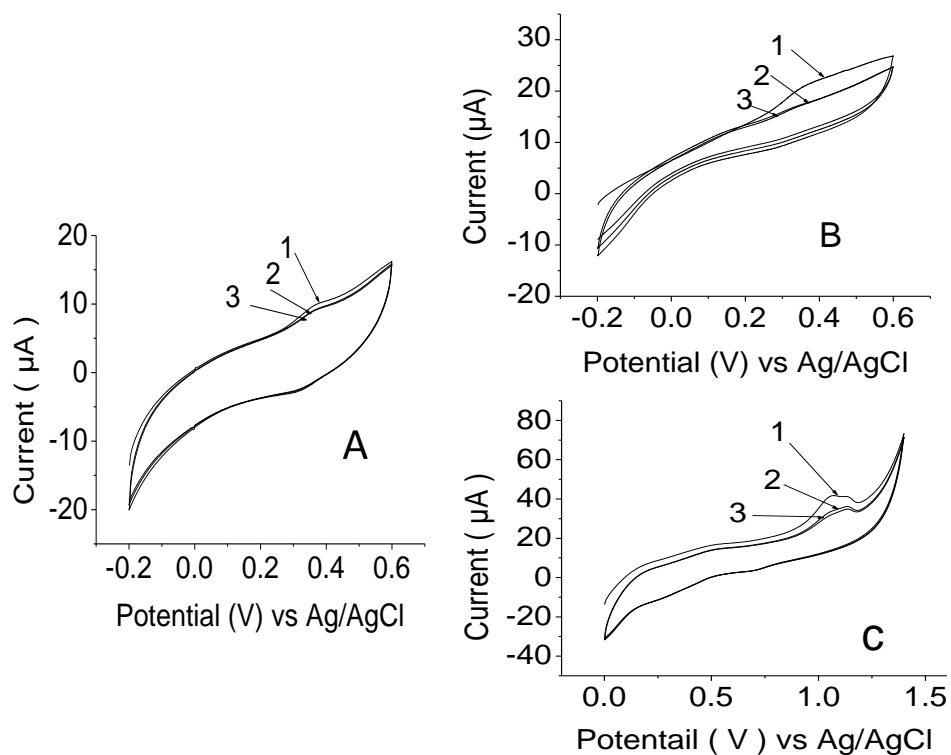


Figure 9. Cyclic voltamogram of grafting of 3 mmol/L p-nitroaniline on (A) bare GCE and (B) AuNPs deposited GCE in 0.5 mol/L HCl ( C ) Cyclic voltamogram of AuNPs nucleated PD modified GCE in 0.1 mol/L KCl for 3 cycles (1, 2, 3 represent first cycle, second cycle and third cycle) in all cases scan rate 100 mV/s

After modifying GCE with AuNPs and grafting p-nitroaniline film, the next step was producing nanoholes. This was achieved by stripping the nucleated AuNPs in 0.1 mol/L KCl using CV from 0 V to 1.4 V with six cyclic scans at a scan rate of 100 mV/s. The anodic peak observed around 0.97 V is due to oxidation of AuNPs. The magnitude of the oxidation peak current decreased in subsequent cycles indicating complete removal of the deposited AuNPs (fig.9 C). The production of nanohole p-nitroaniline grafted glassy carbon electrode (nanohole PNA grafted GCE) was further proved by enhancement of redox peak of  $\text{Ru}(\text{NH}_3)_6\text{Cl}_3$  and HQ, suppression of redox current peak of  $\text{K}_3\text{Fe}(\text{CN})_6$  probe.



### 3.3 Electrochemical Characterization of 4-aminophenol Grafted Nanostructure GCE

#### 3.3.1 Cyclic Voltammetry of $\text{Ru}(\text{NH}_3)_6\text{Cl}_3$

Figure 10 shows CV of  $\text{Ru}(\text{NH}_3)_6\text{Cl}_3$  at bare GCE, Aph grafted GCE and nanohole Aph grafted GCE. Electrochemical response of  $\text{Ru}(\text{NH}_3)_6\text{Cl}_3$  was suppressed at nanohole Aph grafted GCE relative to bare GCE, because  $\text{Ru}(\text{NH}_3)_6^{+3}$  is repelled by Aph film formed on nanostructured electrode which could be electropositive layer.

At Aph grafted GCE redox peak of  $\text{Ru}(\text{NH}_3)_6^{+3}$  suppressed significantly relative to at bare GCE due to uniform monolayer formation Aph film on bare GCE that insulate its surface.

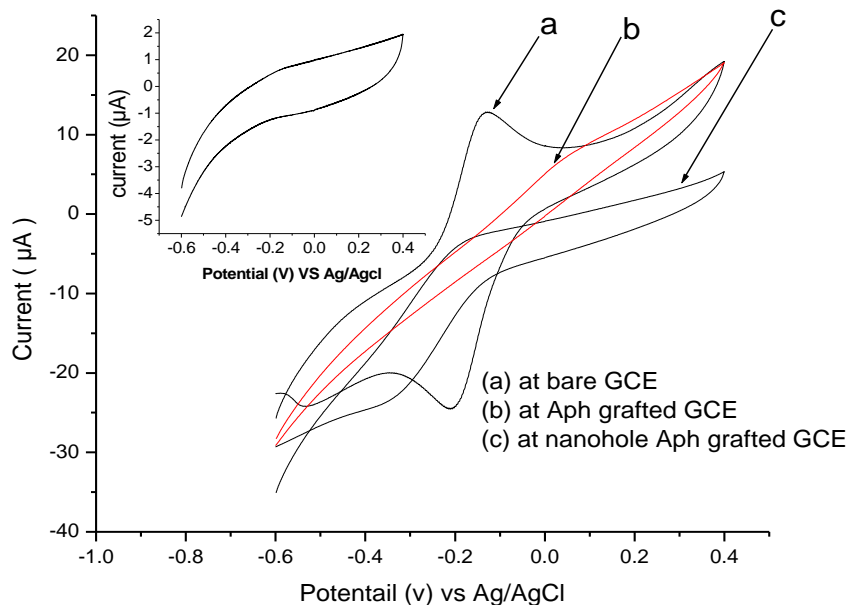


Figure 10. Cyclic voltammogram of 10 mmol/L  $\text{Ru}(\text{NH}_3)_6\text{Cl}_3$  in 0.1 mmol/L  $\text{KNO}_3$ ; (a) at bare GCE (b) Aph grafted GCE (c) nanohole Aph grafted GCE; inset cyclic voltammogram of supporting electrolyte ( 0.1 mmol/L  $\text{KNO}_3$  ) at nanohole Aph grafted GCE in all cases scan rate 50 mV/s

### 3.3.2 Cyclic Voltammetry of $K_3Fe(CN)_6$

Formation of Aph film on GCE checked by running CV of  $K_3Fe(CN)_6$  at Aph grafted GCE. As shown in Figure 11 redox peak of  $K_3Fe(CN)_6$  (electronegative probe) was increased relative to bare GCE; this gave strong evidence of formation of film on GCE which increases electron transfer between ferricyanide and electrode. Redox peaks of ferricyanide at nanohole Aph grafted GCE increased relative to bare and Aph grafted GCE; this is due to electrostatic interaction between the positively charged Aph films with negatively charged ferricyanide and the three dimensional diffusion (3D) of ions toward nanohole electrode are possible reasons for increment of sensitivity of nanohole Aph grafted GCE.

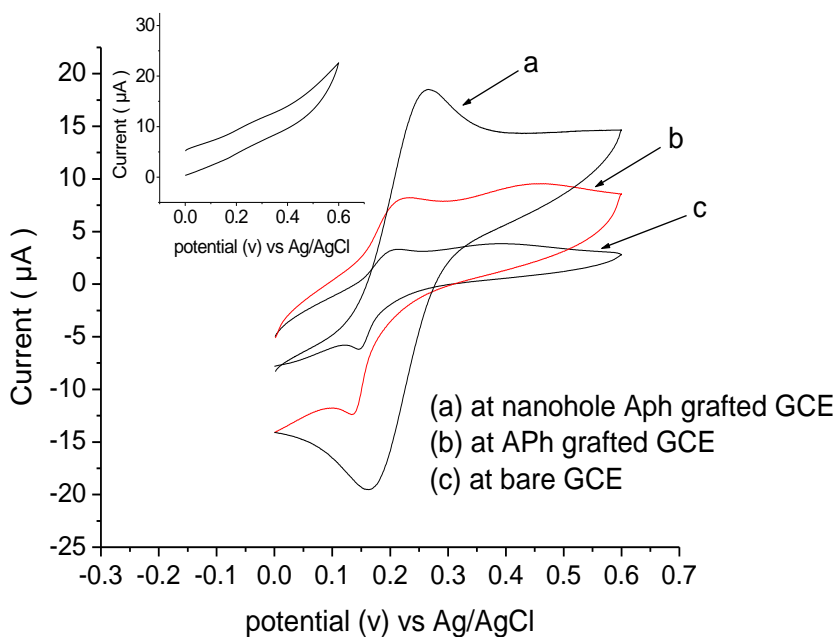


Figure 11. Cyclic voltammogram of 10 mmol/L  $K_3Fe(CN)_6$  in 0.1 mol/L KCl; at (a) nanohole Aph grafted GCE (b) Aph grafted GCE (c) bare GCE; inset cyclic voltammogram of supporting electrolyte (0.1 mol/L KCl) at nanohole Aph grafted GCE, in all cases scan rate 50 mV/s

### 3.3.3 Cyclic Voltammetry of Hydroquinone

Figure 12 depicts the cyclic voltamogram of HQ at bare GCE, nanohole Aph grafted GCE and Aph grafted GCE. Theoretically electrochemical response of HQ is not enhanced by charged modified surface because it is a neutral redox probe; but redox peak increased at nanohole PD grafted GCE due to 3D diffusion toward nanoholes formed relative to bare GCE. Redox peak of HQ decreased at Aph grafted GCE is may be due to Aph film formed decrease active surface of the electrode.

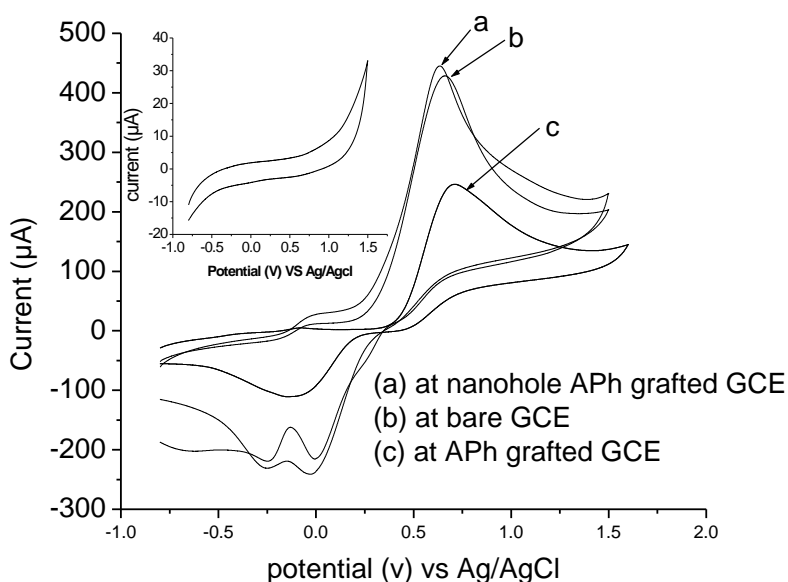


Figure 12. Cyclic voltamogram of 10 mmol/L HQ in 0.1 mol/L NaClO<sub>4</sub>; at (a) nanohole Aph grafted GCE (b) bare GCE and (c) Aph grafted GCE; inset cyclic voltamogram of supporting electrolyte ( 0.1 mol/L NaClO<sub>4</sub>) at nanohole Aph grafted GCE in all cases scan rate 100 mV/s

### 3.3.4 Investigation of Mass Transport of Redox Probes Towards Modified Electrodes

Study of scan rate was made to investigate the mechanism of mass transport of redox probes towards the electrodes. Effect of scan rate on oxidation peak current of K<sub>3</sub>Fe(CN)<sub>6</sub> electronegative and HQ neutral probes were evaluated from 0.05 to 10 Vs<sup>-1</sup> at nanohole Aph grafted GCE and compared to that of bare GCE (Table 1).

Electropositive probe ( $\text{Ru}(\text{NH}_3)_6\text{Cl}_3$ ) was not used in this study as it was repelled by Aph positive film. Anodic peak current against scan rate at both electrodes seems to be overlapped in low scan rates, while it shows good proportionality when scan rate separated from 0.05 to 0.8 V/s and from 1.613 to 10 V/s with respect to  $\text{K}_3\text{Fe}(\text{CN})_6$  probe. This shows diffusion controlled at low scan rate and fast mass transport at high scan rate. A good linear relationship was observed between anodic peak current and square root of the scan rate from 0.05 to 10  $\text{Vs}^{-1}$  with a correlation coefficient of  $R = 0.9987$  and  $R = 0.999$  at bare and nanohole Aph grafted GCE, respectively, demonstrating that the process is more diffusion controlled than other means of mass transport.

Anodic peak current of HQ against scan rate at nanohole Aph grafted GCE and bare GCE is overlapped in low scan rates while it shows good proportionality when scan rates separated from 0.05 to 0.8 v/s and from 1.613 to 10 v/s as in case of  $\text{K}_3\text{Fe}(\text{CN})_6$ . This shows diffusion controlled at low scan rate and fast mass transport at high scan rates. A good linear relationship was observed between the anodic peak current and square root of the scan rate from 0.05 to 10  $\text{Vs}^{-1}$  with a correlation coefficient of  $R = 0.997$  and  $R = 0.998$  at bare and nanohole Aph grafted GCE, respectively, this shows the process is more diffusion controlled than other means of mass transport at both electrodes. Nanoelectrode almost shows the same behavior with bare electrode except enhancement of current peak. This may be due to overlapping of neighboring diffusion layers.

Table1 Effect of scan rate on oxidation peak current of  $K_3Fe(CN)_6$  and HQ at bare and nanohole 4-aminophenol grafted glassy carbon electrode.

Probes	Electrodes	Regression line fitted scan rate		Regression line fitted to square root of scan rate		Range of scan rate in v/s
		Equation	R	Equation	R	
$K_3Fe(CN)_6$	Bare GCE	$Y = 0.03X + 0.06$	0.971	$Y = 0.1X + 0.01$	0.9987	0.05 to 10
	Nanohole Aph grafted GCE	$Y = 0.4X + 0.08$	0.973	$0.14X + 0.002$	0.999	
	Bare GCE	$Y = 0.13X + 0.03$	0.987	$Y = 0.13X + 1.7X10^{-4}$	0.995	0.05 to 0.8
	Nanohole Aph grafted GCE	$Y = 0.11X + 0.03$	0.963	$Y = 0.15 X - 0.004$	0.999	
	Bare GCE	$Y = 0.02X + 0.1$	0.996	$Y = 0.11X - 0.005$	0.9992	1.613 to 10
	Nanohole Aph grafted GCE	$Y = 0.03X + 0.14$	0.995	$Y = 0.14X - 0.01$	0.9999	
HQ	Bare GCE	$Y = 0.19X + 0.498$	0.953	$Y = 0.69X + 0.1$	0.997	0.05 to 10
	Nanohole Aph grafted GCE	$Y = 0.2X + 0.56$	0.954	$Y = 0.71X - 0.15$	0.998	
	Bare GCE	$0.64X + 0.23$	0.983	$Y = 0.74X + 0.056$	0.9997	0.05 to 0.8
	Nanohole Aph grafted GCE	$Y = 0.72X + 0.27$	0.986	$Y = 0.84X + 0.08$	0.9995	
	Bare GCE	$0.14X + 0.87$	0.978	$Y = 0.63X + 0.23$	0.995	1.613 to 10
	Nanohole Aph grafted GCE	$Y = 0.15X + 0.92$	0.988	$Y = 0.667X + 0.25$	0.9988	

### 3.4 Determination of Ascorbic acid at 4-Aminophenol Grafted Nanostructured Glassy Carbon Electrode

4-aminophenol forms positive film on the surface of electrode and it could attract electronegative substance as observed in case of  $K_3Fe(CN)_6$  negative probe. So, determination of AA representing negatively charged analyte done at 4-aminophenol grafted GCE

The oxidation of ascorbic acid ( $C_6H_8O_6$ ) involves two electrons and two protons irreversible reaction to produce dehydroascorbic acid ( $C_6H_6O_6$ ).



As shown in Figure 13 oxidation peak current of AA is enhanced and shifted to lower potential at nanohole Aph grafted GCE relative to that of bare GCE, due to produced nanohole that could change diffusion of ions from planar to three dimensional and also due to electrostatic interaction between negatively charged AA<sup>65, 66</sup> and positively charged 4-aminophenol film. These two factors helped maintain the electrode surface activity through reduced adsorption of the oxidation products, resulting in a more favorable AA oxidation process. Ascorbic acid oxidation at a bare glassy carbon electrode generally occurs at a relatively high oxidation potential, indicating a slow electron transfer rate<sup>101</sup>.

Such sluggish electrode kinetics may also be due to electrode fouling caused by the deposition of oxidation products of AA on the electrode surface. Compton and his coworkers<sup>102</sup> have demonstrated that modifying an electrode with porous layers of conducting material can shift voltammetric peaks, because of a change in the mass-transport regime from planar diffusion to thin-layer character.

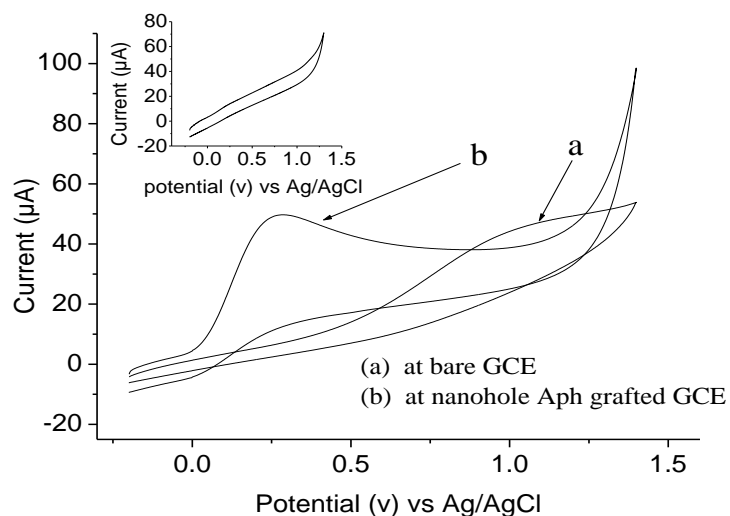


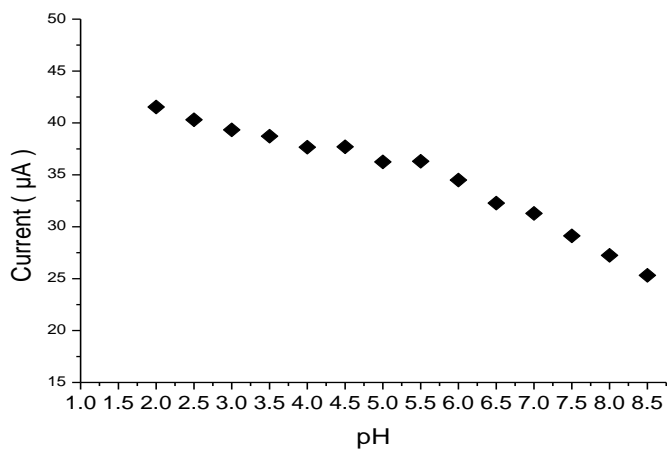
Figure 13. Cyclic voltammogram of 2 mmol/L AA at (a) bare and (b) nanohole Aph grafted GCE in 0.1 mol/L sodium acetate buffer solution; inset Cyclic voltammogram of 0.1 mol/L sodium acetate buffer solution (pH 5) at nanohole Aph grafted GCE in all cases scan rate 100 mV/s

### 3.4.1 Effect of pH on Oxidation Peak Current of Ascorbic Acid

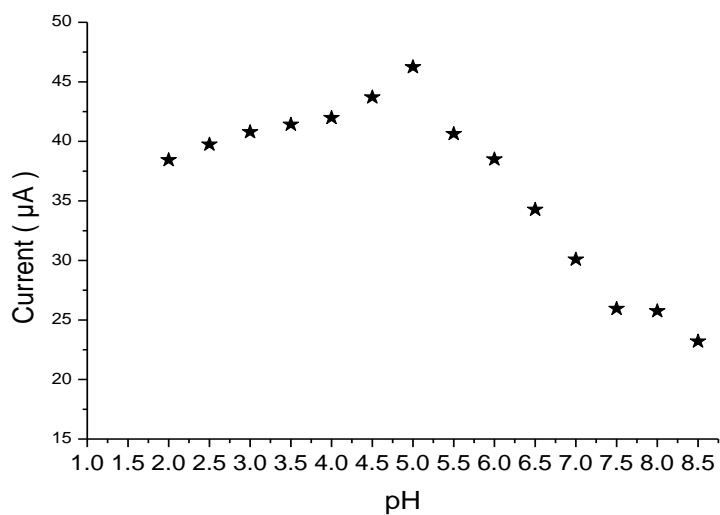
Effect of pH of the supporting electrolyte (buffer) on oxidation peak current of AA was studied within range 2 to 9 using cyclic voltammetry. Citrate buffer was used to study effect of pH within the range of 2 to 4, acetate buffer within the range of 4.5 to 6 and phosphate buffer within the range of 6.5 to 8.5.

As shown in figure 14 oxidation peak current of AA decreased from pH 2 to 9 at bare GCE because AA exists in anionic form <sup>103</sup> and therefore oxidation of AA is favorable at low pH than at high pH. At nanohole Aph grafted GCE oxidation peak current of AA increased in acidic media with pH because AA is attracted by positive film on electrode. From pH 6.5 to 9 oxidation peak current of AA decreased because high pH could neutralize some of the positive charge on the electrode surface and an additional reason could be instability of AA in basic solution; ascorbic acid can be oxidized by dissolved oxygen present as an impurity in solutions and this effect is intensified under alkaline conditions.

Generally oxidation peak current of AA at nanohole Aph grafted GCE increased with increase pH in acidic media and highest sensitivity was observed at pH 5. So, in this work for best of our work we used 0.1 mol/L sodium acetate buffer at pH 5 as electrolyte for determination of ascorbic acid at nanohole Aph grafted GCE.



(i)



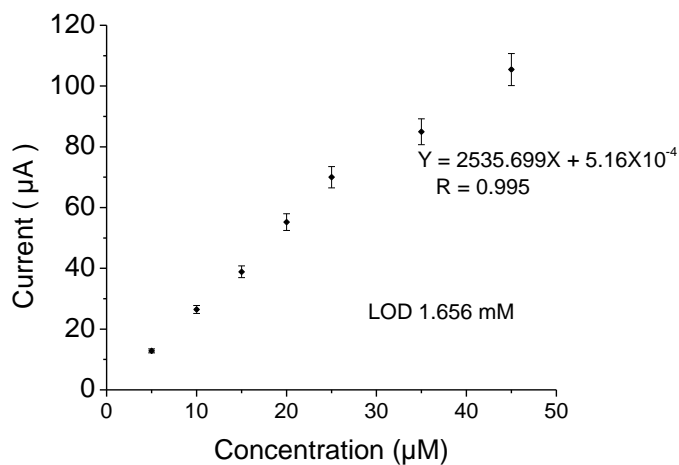
(ii)

Figure 14. Oxidation peak current of 2 mmol/L AA at different pH at (a) bare GCE (b) nanohole Aph grafted GCE

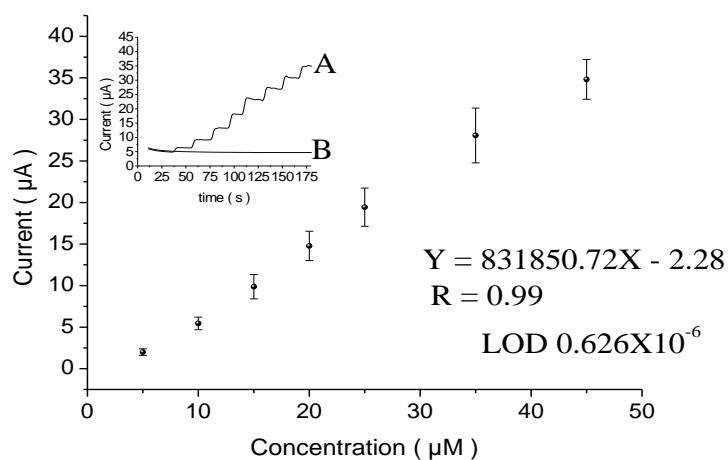


### 3.4.2 Amperometric Response of Ascorbic Acid

Figure 15 displays typical amperometric response of AA at bare and nanohole APh grafted GCE. Amperometric study was carried out through successive addition of 1mmol/L AA into a continuously stirred batch system of 0.1 mol/L acetate buffer (pH 5) at applied potential of 0,8 V and 0.25 V at bare and nanohole APh grafted GCE respectively. A linear relationship was observed between oxidation peak current and concentration of AA in the range  $4 \times 10^{-4}$  to  $2.8 \times 10^{-5}$  mol/L with a correlation coefficient of 0.995 and 0.999 at bare and nanohole APh grafted GCE respectively, demonstrating good relationship between oxidation peak current and concentration. The current values were the average of three measurements for each concentration. Limit of detection ( $LOD = 3\sigma/\text{slope}$ ) at nanohole APh grafted GCE and bare GCE were 0.626  $\mu\text{mol/L}$  and 1.656 mmol/L respectively. The limit of detection at nanohole APh grafted GCE is improved relative to some other previous works <sup>104, 105</sup>(Table 8). These experimental result indicated that nanohole APh grafted GCE has potential application as a chemical sensor for the determination of AA.



(i)



(ii)

Figure 15. Amperometric Calibration curve for determination of AA in acetate buffer ( pH 5) at ( i ) bare GC; (ii) nanohole Aph grafted GCE.; inset (A) amperometric current vs time curve upon successive additions of 1m mol/L AA into a stirred system of 0.1 mol/L sodium acetate buffer (B) amperometric response of buffer only ( pH 5)

### 3.4.3 Effect of Interferent

Interferents such as, caffeine (CAF) and starch (STA) which exists in the pharmaceutical dosages containing vitamin C may influence detection of AA<sup>106</sup>. Substance like glucose (GLU), citric acid (CA) and tartaric acid (TA) may interfere detection of AA in fruit juices<sup>107-109</sup>. In human fluid detection of AA may be interfered by Compounds like glucose (GLU), dopamine (DA) and uric acid (UA)<sup>65, 66, 110</sup>.

As shown in Figure 21 electro oxidation of AA in the presence of above possible interfering substances, under similar conditions was studied using amperometry at 1 mmol/L AA and 1 mmol/L each interfering substance at bare GCE and at fixed concentration of AA (1 mmol/L) and 200-fold excesses of interfering species at nanohole Aph grafted GCE.

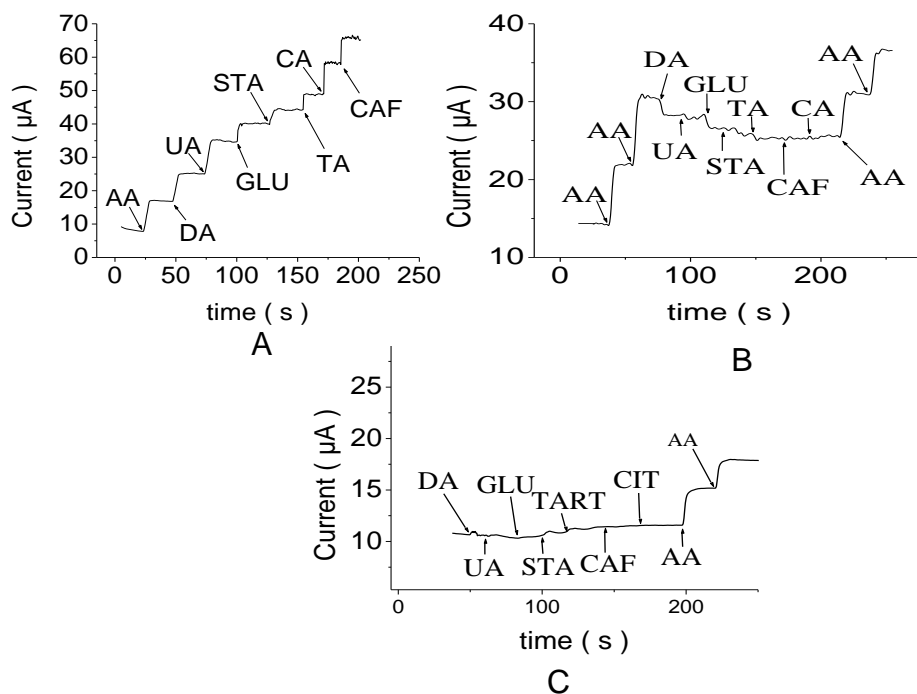


Figure 16. Amperometric response of (A) 1 mmol/L AA and mmol/L interfering species at bare GCE at applied potential of 0.8 V (B) 1 mmol/L AA and 200-fold excesses of interfering species at nanohole Aph grafted GCE at 0.25 V; (C) amperometric response of 1 mmol/L AA and 200-fold excesses of interfering species from interferent to AA at nanohole APH grafted GCE at applied potential of 0.25 V.

Each interfering substances give amperometric response at bare GCE like AA at 0.8 V but amperometric response of AA was not interfered at nanohole Aph grafted GCE by possible interferents at 0.25 V. This is due to electro attraction between electropositive Aph film with electronegative AA and repulsion between film and electropositive substance like DA substance. Other reason could be nanohole Aph grafted GCE specific for oxidation of AA at 0.25 V even though other substance have similar charge with AA or neutral.

### 3.4.4 Real Sample Analysis

Nanohole Aph grafted GCE was applied for determination of AA content in Orange fruit and vitamin C tablet samples. As can be seen from Table 2 and 3 concentration of AA and in Orange fruit and vitamin C tablet at nanohole Aph grafted GCE were  $23.48 \pm 0.47$  mg/100mL and  $503.64 \pm 0.82$  mg/tablet respectively. The concentrations of AA in Orange fruit and vitamin C tablet determined by amperometry are in good agreement with the result obtained by titrimetric method. The result showed that nanohole Aph grafted GCE is good for AA analysis.

Table 2 Determination of AA in orange fruit using nanohole APh grafted GCE

Concentration of ascorbic acid (mg /100mL)		
Titrimetric	At nanohole APh grafted GCE	% error
$23.33 \pm 0.01$	$23.48 \pm 0.47$	0.64

Table 3 Determination of AA in vitamin C tablet using nanohole PD grafted GCE

Concentration of ascorbic acid (mg per tablet)		
Titrimetric	At nanohole APh grafted GCE	% error
$504.97 \pm 0.03$	$506.31 \pm 0.82$	0.26

Mean  $\pm$  SD, n = 3 for each sample

### **3.5 Stability and Reproducibility of Nanohole 4-Aminophenol Grafted Glassy Carbon Electrode**

Nanohole APh grafted GCE was fabricated according to the optimized condition and stored in 0.1mol/L citrate buffer (pH 5) at room temperature, and the stability of modified electrode was tested on 28 days at 2 mmol/L AA and the peak current of AA retained 96% of its initial current response. The result showed that nanohole APh grafted GCE has a good stability and long life. Five nanohole APh grafted GCEs were prepared under the same preparing conditions in different day and the peak current of 2 mmol/L AA was measured in each case. The relative standard deviation of peak current was 5.21% (n=5), showing good reproducibility of the modified electrode.

### 3.6 Electrochemical Characterization of p-Phenylenediamine Grafted Nanostructure Glassy Carbon Electrode

P-phenylenediamine forms positively charged film on the surface of GCE in acidic media. So, it could attract anionic substances to the surface of electrode and thereby enhancing their redox peak. In other case, it could repel cationic substances and suppresses their redox peak. In this work  $\text{Ru}(\text{NH}_3)_6\text{Cl}_3$  (cationic),  $\text{K}_3\text{Fe}(\text{CN})_6$  (anionic) and HQ (neutral) probes were used to characterize the modified electrode.

#### 3.6.1 Cyclic Voltammetry of $\text{Ru}(\text{NH}_3)_6\text{Cl}_3$

Figure 17 depicts the CV of  $\text{Ru}(\text{NH}_3)_6\text{Cl}_3$  at bare, PD grafted GCE and at nanohole PD grafted GCE. Electrochemical response of  $\text{Ru}(\text{NH}_3)_6\text{Cl}_3$  suppressed at nanohole PD grafted GCE relative to at bare GCE because  $\text{Ru}(\text{NH}_3)_6^{+3}$  is repelled by PD positive film formed on the nanostructured electrode. At PD grafted GCE redox peak of  $\text{Ru}(\text{NH}_3)_6^{+3}$  is diminished due to uniform monolayer PD film formed on GCE that insulate its surface.

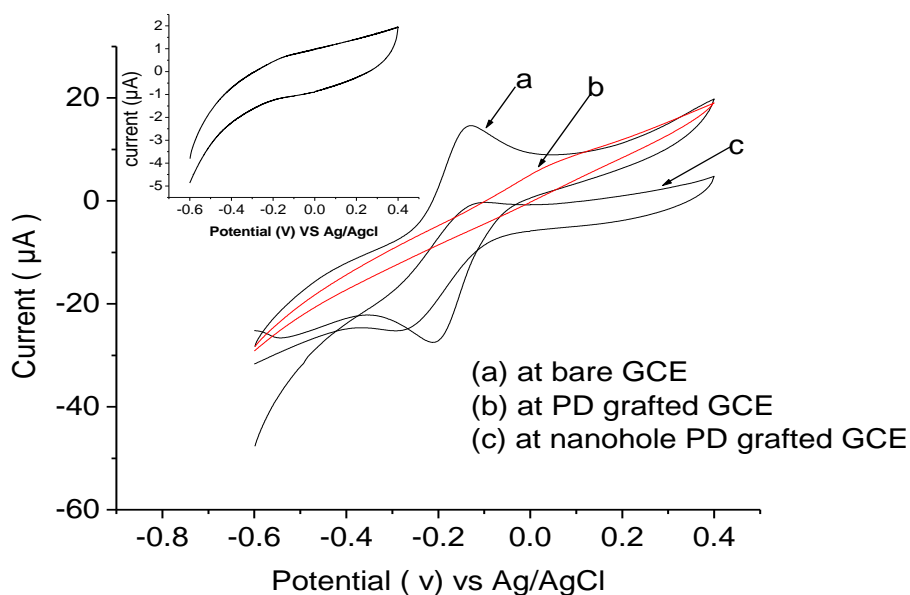


Figure 17. Cyclic Voltammogram of 10 mmol/L  $\text{Ru}(\text{NH}_3)_6\text{Cl}_3$  in 0.1 mol/L  $\text{KNO}_3$  at (a) bare GCE, (b) PD grafted GCE, (c) nanohole PD grafted GCE, inset Cyclic voltammogram of 0.1 mol/L  $\text{KNO}_3$  using nanohole PD grafted GCE. Scan rate 50 mV/s in all cases.

### 3.6.2 Cyclic Voltammetry of $K_3Fe(CN)_6$

Figure 18 depicts the CV of  $K_3Fe(CN)_6$  at bare, PD grafted GCE and nanohole PD grafted GCE. Redox peak of  $K_3Fe(CN)_6$  enhanced at PD grafted GCE relative to at bare GCE, because cationic film PD increase electron transfer by attracting ferricyanide ion toward surface of electrode. Redox peak current of ferricyanide at nanohole PD grafted GCE is enhanced compared to that of bare and PD grafted GCE; this is due to electrostatic interaction between the positively charged film PD with negatively charged ferricyanide and 3D diffusion of ions toward nanoelectrodes.

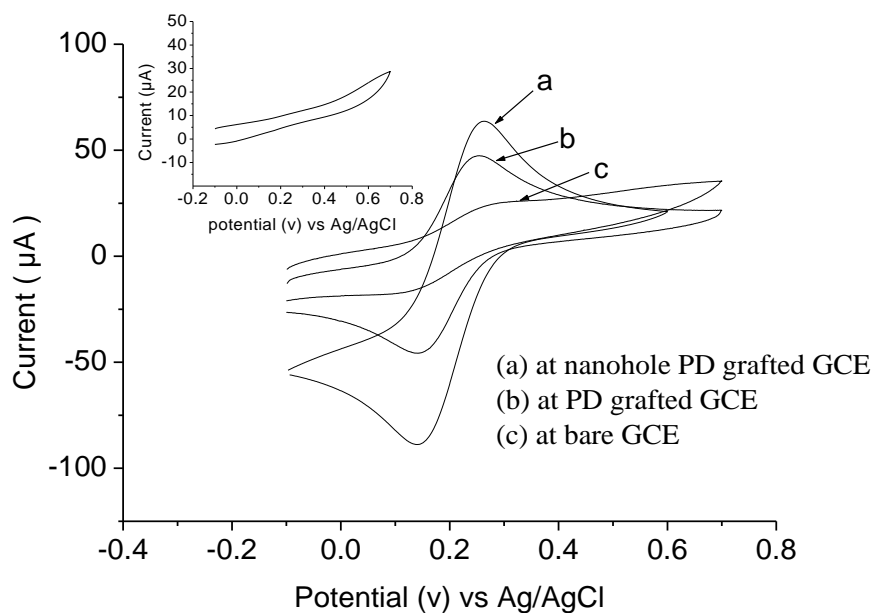


Figure 18. Cyclic voltammogram of 10 mmol/L  $K_3Fe(CN)_6$  in 0.1 mol/L KCl at (a) nanohole PD grafted GCE, (b) PD grafted GCE, (c) bare GCE, inset Cyclic voltammogram of 0.1 mol/L KCl using nanohole PD grafted GCE. Scan rate 50 mV/s in all cases

### 3.6.3 Cyclic Voltammetry of Hydroquinone

Figure 19 shows cyclic voltamogram of HQ at bare GCE, nanohole PD grafted GCE and PD grafted GCE. Theoretically electrochemical response of HQ should not be affected by positive or negative charged films formed on electrodes; because HQ is neutral and is not attracted nor repulsed by charged films; but at nanohole PD grafted GCE redox peak of HQ increased relative to at bare GCE, due to holes formed at modified electrode that could change diffusion from planar to 3D. At PD grafted GCE redox peak suppressed relative to bare GCE, due to decrease of electrode active surface by the film formed.

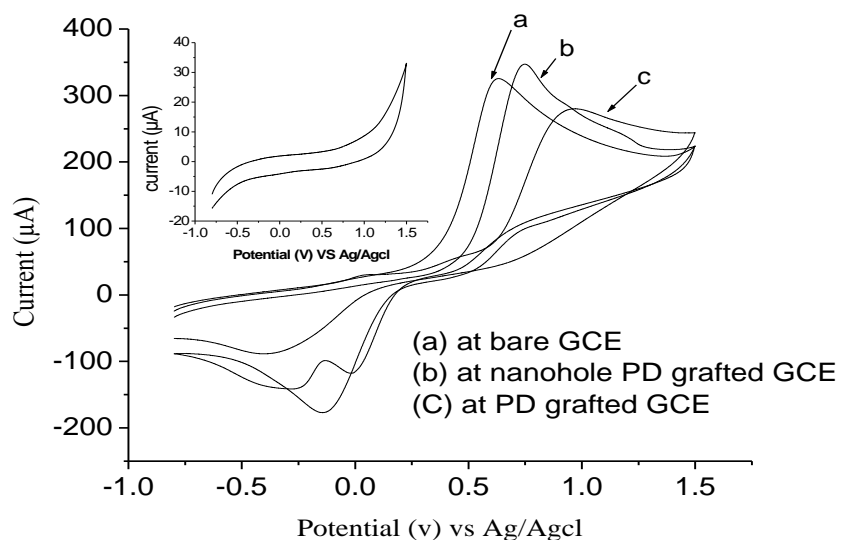


Figure 19. Cyclic voltamogram of 10 mmol/L HQ in 0.1 mol/L NaClO<sub>4</sub> at (a) bare GCE, (b) nanohole PD grafted GCE, (c) PD grafted GCE; Inset cyclic voltamogram of supporting electrolyte (0.1 mol/L NaClO<sub>4</sub>), scan rate 100 mV/s in all cases.



### 3.6.4 Effect of Scan Rate on Oxidation Peak Current of $K_3Fe(CN)_6$ and Hydroquinone Probes

The effect of scan rate on oxidation peak current of  $K_3Fe(CN)_6$  and HQ was studied from low to high scan rate at nanohole PD grafted GCE and compared to that of bare GCE.  $Ru(NH_3)_6Cl_3$  was not selected to study the effect of scan rate as it was repulsed by PD film. As can be observed from Table 4, the effect of scan rate on oxidation peak current of  $K_3Fe(CN)_6$  was evaluated from 0.05 to 10 V/s at bare GCE and nanohole PD grafted GCE. Graph of anodic peak current against scan rate of  $K_3Fe(CN)_6$  at nanohole PD grafted GCE and bare GCE is overlapped in low scan rates while it shows good proportionality when scan rate separated from 0.05 to 0.8 V/s and from 1.613 to 10 V/s. This shows diffusion controlled at low scan rate and fast mass transport at high scan rate. The peak current have shown a better linearity with square root of scan rate at low scan rate from 0.05 to 0.8 V/s with correlation coefficient of  $R= 0.990$  and  $R= 0.999$ , and from 1.613 to 10 V/s with correlation coefficient of  $R= 0.999$ , and  $R= 0.995$  at bare and nanohole PD grafted GCE respectively. This result show the process is more diffusion controlled at bare GCE and fast mass transport at nanohole PD grafted GCE at high scan rate.

Anodic peak current of HQ against scan rate at nanohole PD grafted GCE and bare GCE is overlapped in low scan rates while it shows good proportionality when scan rates separated from 0.05 to 0.8 v/s and from 1.613 to 10 v/s as in case of  $K_3Fe(CN)_6$ . This shows diffusion controlled at low scan rate and fast mass transport at high scan rate. A good linear relationship was observed between anodic peak current and square root of scan rate. The relationship is better at nanohole PD grafted GCE than at bare GCE in all cases demonstrating that the process is diffusion controlled at nanohole PD grafted GCE and adsorption controlled at bare GCE.

Table 4 Effect of scan rate on oxidation peak current of  $K_3Fe(CN)_6$  and HQ at bare and nanohole p- phenylenediamine grafted glassy carbon electrode.

Probes	Electrodes	Regression line fitted scan rate		Regression line fitted to square root of scan rate		Range of scan rate (v/s)
		Equation	R	Equation	R	
$K_3Fe(CN)_6$	Bare GC	$Y = 0.03X + 0.06$	0.971	$Y = 0.1X + 0.01$	0.9987	0.05 to 10
	Nanohole PD grafted GC	$Y = 0.04X + 0.09$	0.954	$0.15X + 0.01$	0.998	
	Bare GC	$Y = 0.13X + 0.03$	0.987	$Y = 0.13X + 1.7X10^{-4}$	0.995	0.05 to 0.8
	Nanohole PD grafted GC	$Y = 0.13X + 0.04$	0.986	$Y = 0.15X + 0.001$	0.999	
	Bare GC	$Y = 0.02X + 0.1$	0.996	$Y = 0.11X - 0.005$	0.999	1.613 to 10
	Nanohole PD grafted GC	$Y = 0.03X + 0.15$	0.984	$Y = 0.14X + 0.14$	0.995	
HQ	Bare GC	$Y = 0.19X + 0.498$	0.953	$Y = 0.69X + 0.1$	0.997	0.05 to 10
	Nanohole PD grafted GC	$Y = 0.25X + 0.63$	0.953	$Y = 0.86X + 0.14$	0.998	
	Bare GC	$0.64X + 0.23$	0.983	$Y = 0.74X + 0.056$	0.9997	0.05 to 0.8
	Nanohole PD grafted GC	$Y = 0.81X + 0.23$	0.966	$Y = 0.74X + 0.056$	0.999	
	Bare GC	$0.14X + 0.88$	0.978	$Y = 0.63X + 0.23$	0.995	1.613 to 10
	Nanohole PD grafted GC	$Y = 0.18X + 1.1$	0.982	$Y = 0.81X + 0.26$	0.996	

### **3.7 Determination of Ascorbic Acid at p-Phenylenediamine Grafted Nanostructured Glassy Carbon Electrode**

Ascorbic acid is electronegative analyte and p-phenylenediamine forms cationic film on the surface of glassy carbon electrode. So, p-phenylenediamine film grafted nano structured GCE used for ascorbic acid analysis.

Oxidation of AA involves two electrons and two protons irreversible reaction to produce dehydroascorbic acid (equation 8.1). As shown in figure 20 Oxidation peak current of AA is enhanced and shifted to lower oxidation potential at nanohole PD grafted GCE relative to at bare GCE. The enhanced response is attributed to the electrostatic interaction between negatively charged AA and positively charged PD film. This maintains the electrode surface activity through reduced adsorption of the oxidation products, resulting in a more favorable AA oxidation process.

Oxidation of AA at a bare GCE generally occurs at a relatively high oxidation potential, indicating a slow electron transfer rate at bare GCE<sup>101</sup>. Such sluggish electrode kinetics may be also due to electrode fouling caused by the deposition of oxidation product of AA on the electrode surface. Compton and his coworkers<sup>102</sup> have demonstrated that modifying an electrode with porous layers of conducting material shifts voltammetric peaks, because of a change in the mass-transport regime from planar diffusion to thin-layer character.

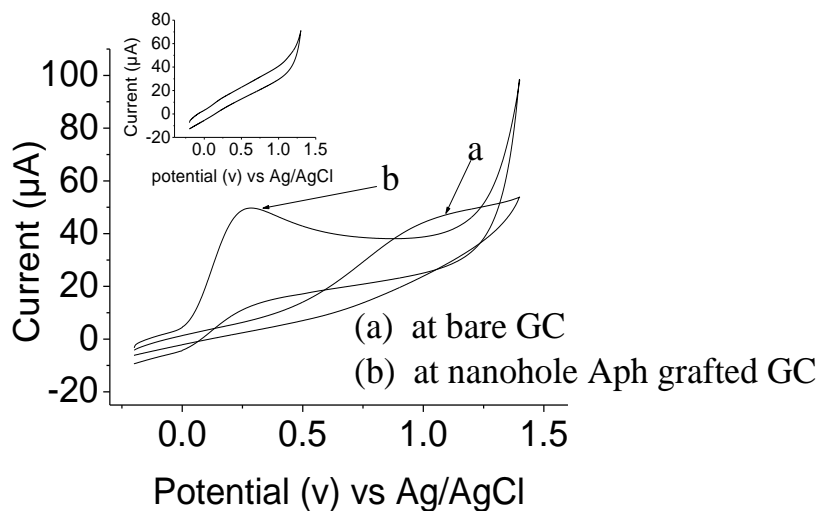


Figure 20. Cyclic voltammogram of 2 mmol/L AA in 0.1 mol/L sodium acetate buffer, at (a) bare and (b) nanohole PD grafted GCE. Inset: cyclic voltammogram of supporting electrolyte (0.1 mol/L sodium acetate buffer) at nanohole PD grafted GCE. In all cases (pH 5) and scan rate 100 mV/s

Figure 21 depict cyclic voltammogram of AA at nanohole PD grafted GCE, nanohole Aph grafted GCE, nanohole PNA grafted GC and at bare GCE. Enhancement of redox peak at nanohole PD grafted GCE relative to at nanohole Aph grafted GCE is due to more electro positivity of (more electron donating tendency) of  $\text{NH}_2$  group of PD than OH group of APh that attract negatively charged AA toward nanostructured electrodes. At nanohole PNA grafted GCE less oxidation peak observed is due to charge repulsion between negatively charged PNA film and ascorbic acid.

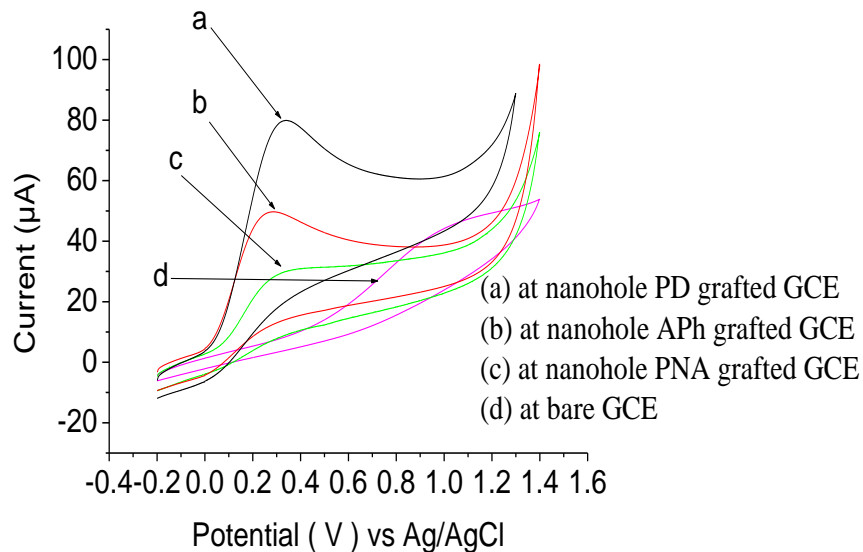
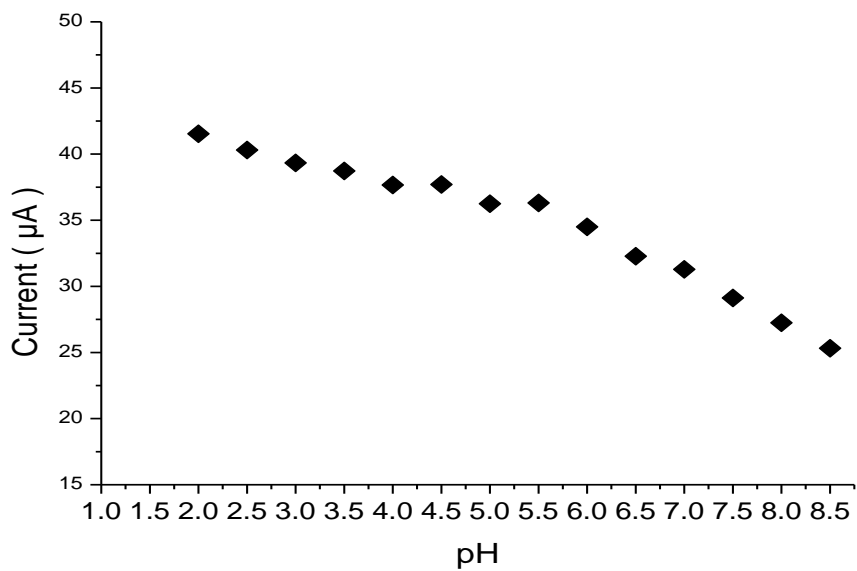


Figure 21. Cyclic voltammogram of 2 mmol/L AA in 0.1 mol/L in sodium acetate ( buffer pH5 ) solution at (a) nanohole PD grafted GCE, (b) nanohole APh grafted GCE, (c) nanohole PNA grafted GCE and (d) bare GCE in all cases scan rate 100 mV/s

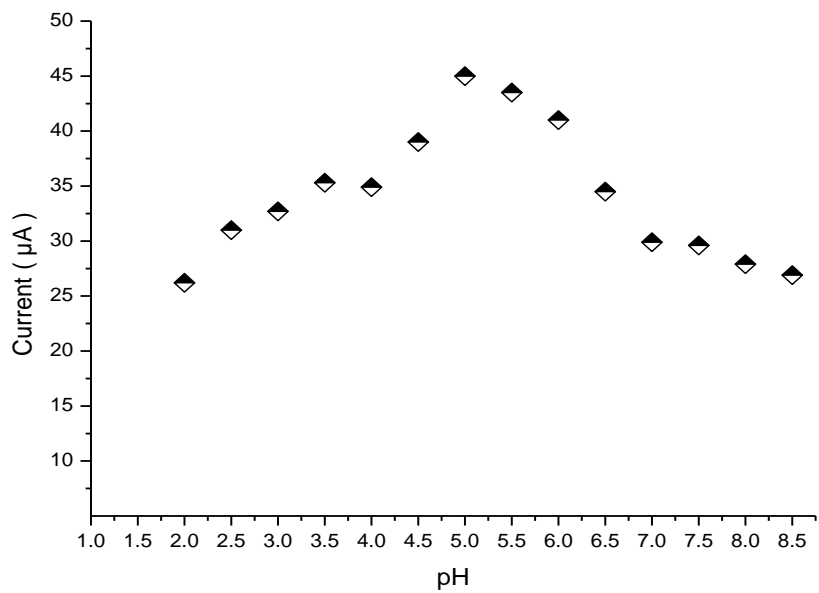
### 3.7.1 Effect of pH on Oxidation Peak Current of Ascorbic Acid

Effect of pH of the supporting electrolyte (buffer) on oxidation peak current of AA was studied within range 2 to 9. Citrate buffer was used to study effect of pH within the range of 2 to 4, acetate buffer was used within range of 4.5 to 6 and phosphate buffer was used within the range 6.5 to 8.5.

As shown in figure 22 oxidation peak current of AA decreased from pH 2 to pH 8.5 at bare GCE, because AA exists in anionic form<sup>103</sup> and therefore oxidation of AA favorable at low pH than at high pH. At nanohole PD grafted GCE oxidation peak current of AA increased from pH 2 to 4 showing maximum peak at pH 5 and decreased from pH 6.5 to 8.5. Oxidation peak current of AA in acidic media was higher than that in basic media this is due to attraction of ascorbate ion to positive film in acidic media<sup>99</sup>. In basic media oxidation peak current of AA is less than that in acidic media this could be due to neutralization of positive film and instability of AA in basic solution. So, for best of our work sodium acetate buffer at pH 5 was selected as electrolyte in this work.



(i)

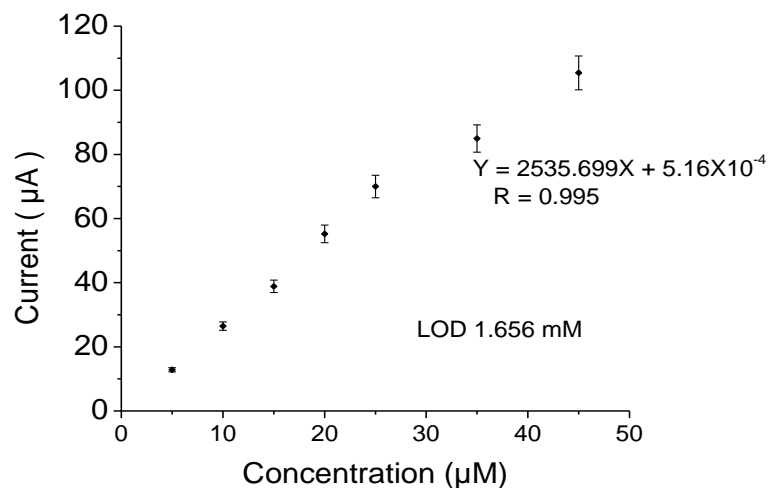


(ii)

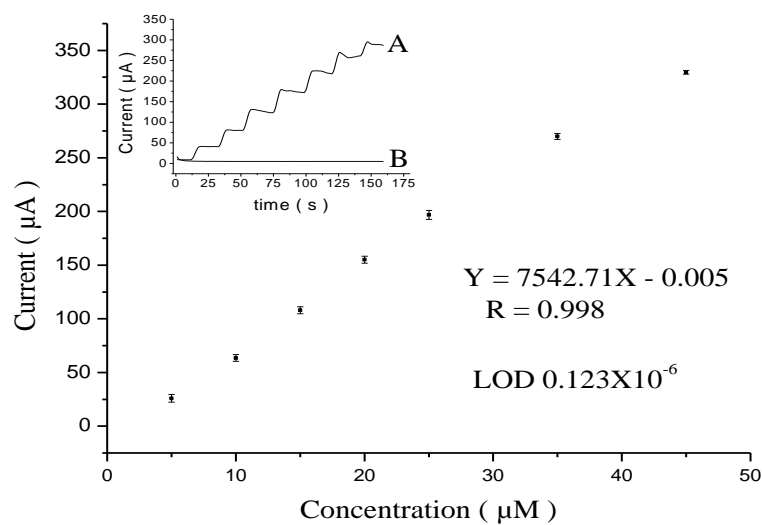
Figure 22. Oxidation peak current of 2 mol/L AA in different pH supporting electrolyte at (i) bare GCE (ii) nanohole PD grafted GCE

### 3.7.2 Amperometric Response of Ascorbic Acid

Figure 23 displays typical amperometric response of AA at bare GCE and nanohole PD grafted GCE for varying concentration of AA. Amperometric study was carried out through successive addition of 1mmol/L AA into a continuously stirred batch system of 0.1 mol/L acetate buffer (pH 5) at applied potential of 0.8 V and 0.237 V at bare and nanohole PD grafted GCE respectively. A linear relationship was observed between oxidation peak current and concentration of AA with a correlation coefficient of 0.998 and 0.995 at nanohole PD grafted GCE and bare GCE respectively, demonstrating good relationship between oxidation peak current and concentration. The limit of detection at nanohole PD grafted GCE and at bare GCE were 0.123 $\mu$  mol/L and 1.656 m mol/L respectively. Limit of detection of nanohole PD grafted GCE is improved relative to some other previous works<sup>104, 105</sup>(Table 8), which shows nanohole PD grafted GCE can use for determination of very low concentration of AA in real sample. The current values were the average of three measurements for each concentration.



(i)



(ii)

Figure 23. Calibration curve for determination of AA at (i) bare GCE (ii) nohole PD grafted GCE; inset (A) amperometric current vs. time curve upon successive additions of 1mmol/L AAs into a stirred system of 0.1 mol/L sodium acetate buffer (pH 5) volume of original solution ( B) amperometric curve for the buffer only (pH 5).



### 3.7.3 Effect of Interferent

The influence of possible interferences, such as, caffeine (CAF), starch (STA) which exists in the pharmaceutical dosages containing vitamin C<sup>106</sup>, glucose (GLU), citric acid (CA) and tartaric acid (TA) which may exist in fruit juices<sup>107-109</sup> and compounds like glucose (GLU), dopamine (DA) and uric acid (UA) which exists in human fluid<sup>65, 66, 110</sup> may interfere detection of AA.

Electro-oxidation of AA in the presence of above possible interfering substances, under similar conditions was studied using amperometry at pH 5 at 1 mmol/L AA and 1 mmol/L each interfering substances at bare GCE at 0.8 V. Electro-oxidation of AA in the presence of above possible interfering substances, under similar conditions was studied at a fixed concentration of 1 mmol/L AA and 200-fold excesses of interfering species at nanohole PD grafted GCE.

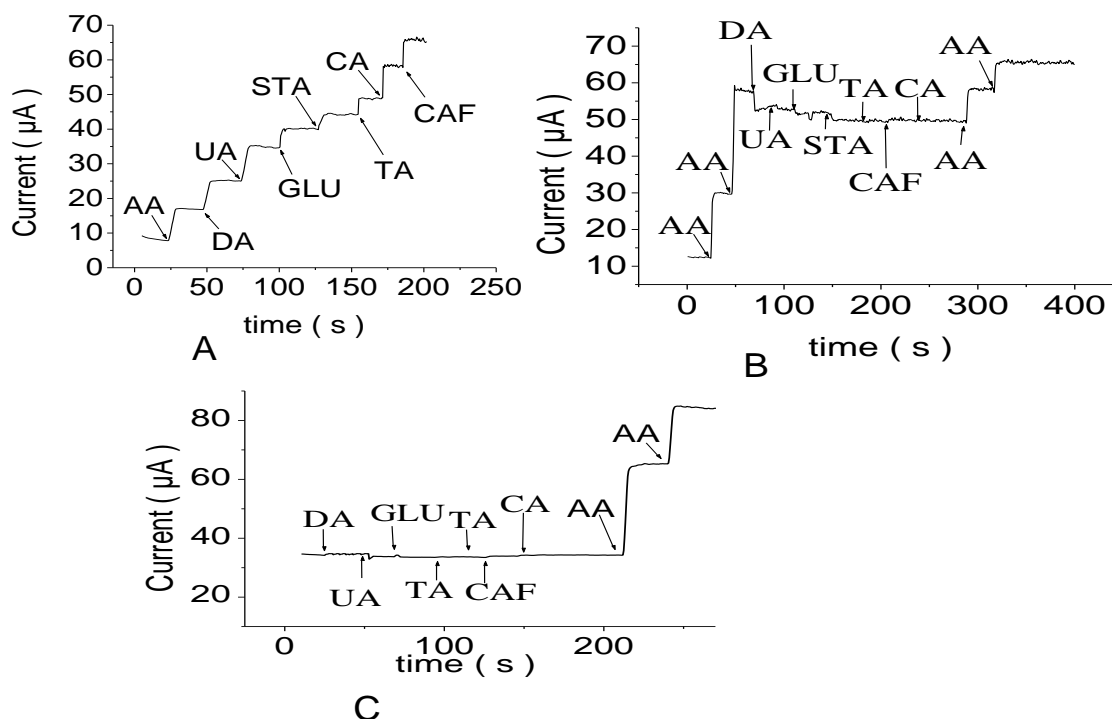


Figure 24. Amperometric response of (A) 1 mmol/L AA and mmol/L interfering species at bare GCE at 0.8 V (B) 1 mmol/L AA and 200-fold excesses of interfering species at nanohole PD grafted GCE at 0.237 V; (C) amperometric response of 1 mmol/L AA and 200-fold excesses of interfering species from interferent to AA at nanohole PD grafted GCE at 0.237 V.

As can be seen from Figure 24, amperometric response of AA was interfered at bare GCE and not interfered at nanohole PD grafted GCE by possible interferents at selected potentials. This is due attraction between positive film and AA and repulsion with positive substance like DA. Even though other substances have similar charge with AA or neutral, at nanohole PD grafted GCE only AA is oxidized at 0.237 V.

### 3.7.4 Real sample Analysis

As can be seen from Table 5 concentration of AA in Orange fruit at nanohole PD grafted GCE was  $23.34 \pm 0.17$  mg/100mL. In vitamin C tablet concentration of AA determined at nanohole PD grafted GCE was  $506.87 \pm 0.39$  mg/tablet (Table 6). Concentrations of AA in Orange fruit and Vitamin C tablet determined by amperometry are in good agreement with the result obtained by titrimetric method. The result showed nanohole PD grafted GCE is good for AA analysis.

Table 5 Determination of AA in orange fruit using nanohole PD grafted GCE

Concentration of ascorbic acid (mg /100mL)			
Titrimetric	Amperometric		% error
$23.33 \pm 0.01$	At nanohole PD grafted GCE	$23.34 \pm 0.17$	0.04

Table 6 Determination of AA in vitamin C tablet using nanohole PD grafted GCE

Concentration of ascorbic acid(mg/ per tablet)			
Titrimetric	Amperometric		% error
$504.97 \pm 0.03$	At nanohole PD grafted GCE	$506.87 \pm 0.39$	0.37

Mean  $\pm$  SD, n = 3 for each sample

### **3.7.5 Stability and Reproducibility of Nanohole p-Phenylenediamine Grafted Glassy Carbon Electrode**

Nanohole PD grafted GCE was prepared according to the optimized condition and stored in 0.1 mol/L citrate buffer (pH 5) at room temperature. The stability of modified electrode was tested after 28 days since it was fabricated using AA; the peak current of 2 mmol/L AA retained 98% of its initial response. The result showed that nanohole PD grafted GCE has a good stability and long life. Five nanohole PD grafted GCE were prepared under the same preparing conditions and the peak current of AA measured at each fabricated electrode. The relative standard deviation of peak current was 5.18% (n=5), showing good reproducibility of the modified electrode.

### 3.8 Electrochemical Characterization of p-Nitroaniline Grafted Nanostructured Glassy Carbon Electrode

P-nitroaniline forms negative film on GCE therefore it could attract cationic substance and repel anionic substance. In this work  $K_3Fe(CN)_6$  (anionic),  $Ru(NH_3)_6Cl_3$  (cationic) and hydroquinone (neutral) probes were selected to characterize the modified electrodes by p-nitroaniline film.

#### 3.8.1 Cyclic Voltammetry of $K_3Fe(CN)_6$

Formation p-nitroaniline film on glassy carbon electrode was checked by running cyclic voltamogram of  $K_3Fe(CN)_6$  at p-nitroaniline grafted glassy carbon electrode(PNA grafted GCE). As can be seen from Figure 25 redox peak of  $K_3Fe(CN)_6$  significantly suppressed at nanohole PNA grafted GCE relative to at bare GCE, this is due to repulsion effect between negatively charged PNA film and negatively charged ferricyanide ion. At PNA grafted GCE redox peak of  $K_3Fe(CN)_6$  totally disappeared because GCE is insulated by PNA film.

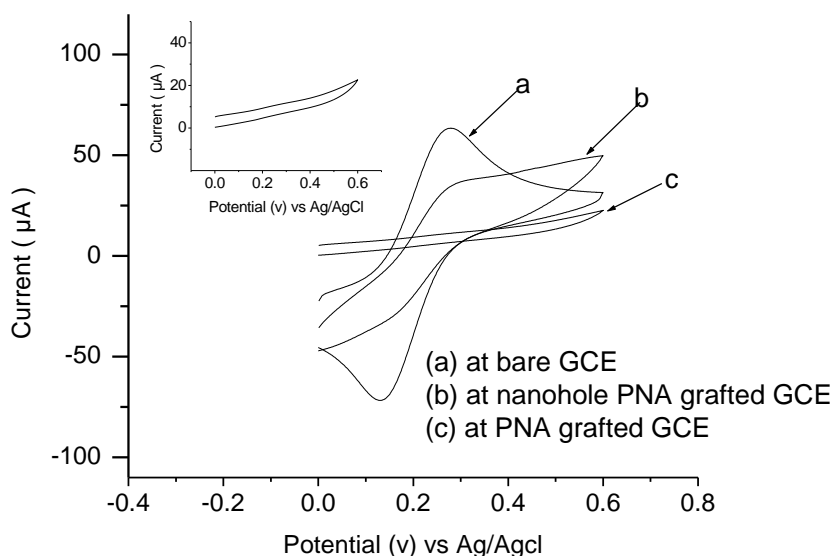


Figure 25. Cyclic voltamogram of 10 mmol/L  $K_3Fe(CN)_6$  in 0.1 mol/L KCl at (a) bare GCE (b) nanohole PNA grafted GCE (c) PNA grafted GCE; Inset cyclic voltamogram of supporting electrolyte (0.1 mol/L KCl); in all cases scan rate 50 mV/s

### 3.8.2 Cyclic Voltammetry of $\text{Ru}(\text{NH}_3)_6\text{Cl}_3$

Formation of P-nitroaniline film on GCE was checked by running cyclic voltamogram of  $\text{Ru}(\text{NH}_3)_6\text{Cl}_3$  (Figure 26). Redox peak of  $\text{Ru}(\text{NH}_3)_6\text{Cl}_3$  enhanced at PNA grafted GCE relative to that of at bare GCE; this is due to PNA film assist fast electron transfer to electrode surface. At nanohole PNA grafted GCE electrochemical response of  $\text{Ru}(\text{NH}_3)_6^{+3}$  enhanced significantly due to electroattraction between PNA film and cationic  $\text{Ru}(\text{NH}_3)_6^+$  and three dimensional diffusion of ion toward nanohole electrode.

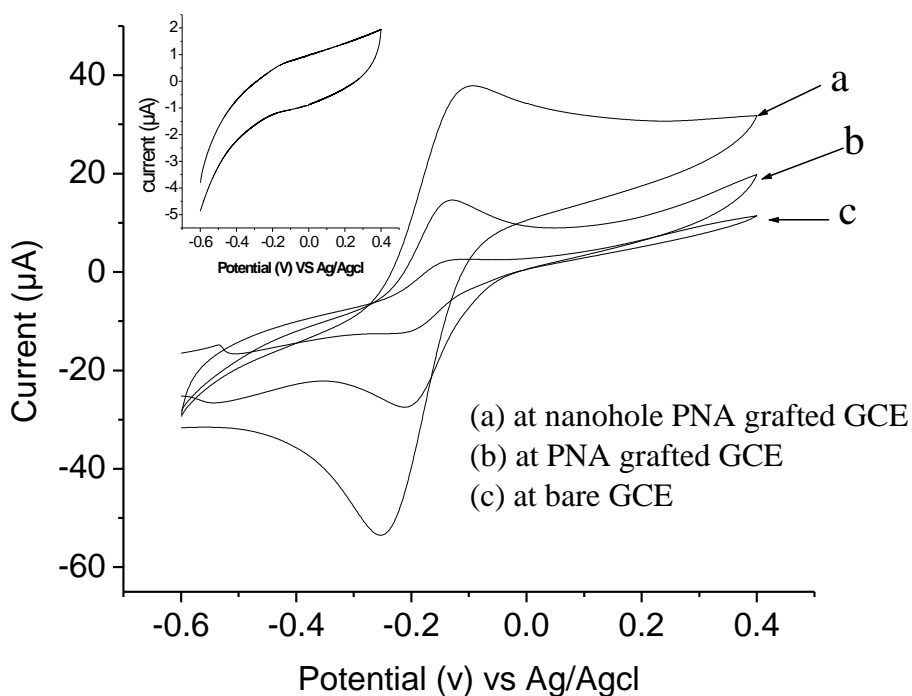


Figure 26. Cyclic Voltamogram of 10 mmol/L  $\text{Ru}(\text{NH}_3)_6\text{Cl}_3$  in 0.1 mol/L  $\text{KNO}_3$ ; at (a) nanohole PNA grafted GCE, (b) PNA grafted GCE and (c) bare GCE; Inset Cyclic voltamogram of nanohole PNA grafted GCE in blank supporting electrolyte (0.1 mol/L  $\text{KNO}_3$ ) at 50 mV/s in all cases

### 3.8.3 Cyclic Voltammetry of Hydroquinone

Figure 27 shows Cyclic Voltamogram of HQ at nanohole PNA grafted GCE, PNA grafted GCE and bare GCE. Electrochemical response of hydroquinone is not affected both by positive and negative charged films formed on nanohole electrodes; because HQ is a neutral in charge. But at nanohole PNA grafted GCE redox peak was enhanced due to 3D diffusion to nanohole electrodes and at PNA grafted GCE redox peak suppressed due to PNA film formed on electrode reduces active areas of the electrode.

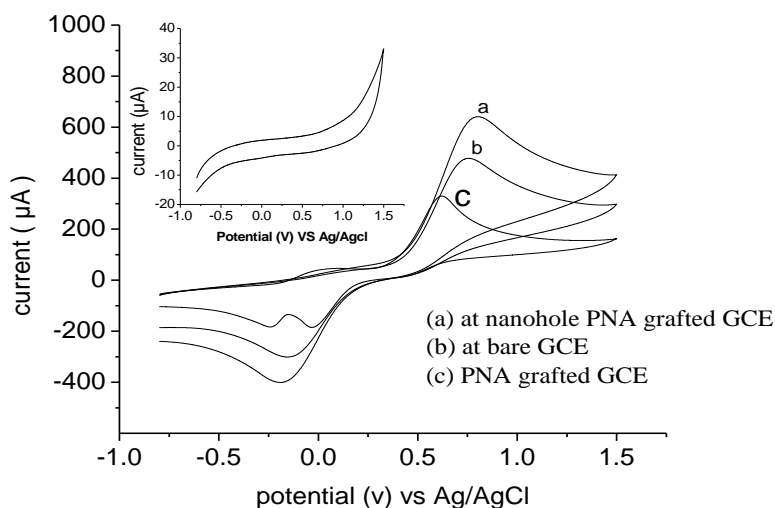


Figure 27. Cyclic Voltammogram of 10 mmol/ L HQ in 0.1mol/L NaClO<sub>4</sub>; at (a) nanohole PNA grafted GCE , (b) bare GCE and (c) PNA grafted GCE; Inset Cyclic Voltammogram of nanohole PNA grafted GCE in supporting electrolyte (0.1mol/L NaClO<sub>4</sub>) at 50 mV/s in all cases

### 3.8.4 Effect of Scan Rate on Oxidation Peak Current of Ru (NH<sub>3</sub>)<sub>6</sub>Cl<sub>3</sub> and Hydroquinone

As we have seen in the above section oxidation peak current of Ru(NH<sub>3</sub>)<sub>6</sub>Cl<sub>3</sub> (electropositive) and HQ (neutral) probes enhanced where as oxidation peak current of K<sub>3</sub>Fe(CN)<sub>6</sub> (electronegative) probe suppressed at nanohole PNA grafted GCE. Therefore Ru(NH<sub>3</sub>)<sub>6</sub>Cl<sub>3</sub> and HQ probes were selected to study effect of scan rate on oxidation peak current at nanohole PNA grafted GCE

As can be seen from Table 7, the effect of scan rate on oxidation peak current of  $\text{Ru}(\text{NH}_3)_6\text{Cl}_3$  and HQ was studied at nanohole PNA grafted GCE and compared to that of bare GCE from 0.05 to 10 V/s. Oxidation peak current vs scan rate of  $\text{Ru}(\text{NH}_3)_6\text{Cl}_3$  at bare GCE and nanohole PNA grafted GCE increases with increasing scan rate. Relation of oxidation peak current to scan rate seemed to be overlapped in low scan rate and shows good proportionality when scan rate separated from 0.05 to 0.8v/s and from 1.613 to 10v/s. This shows diffusion controlled at low scan rate and fast mass transport at high scan rate. A good linear relationship was observed between the anodic peak current and square root of the scan rate from 0.05 to 10  $\text{Vs}^{-1}$  with a correlation coefficient of  $R= 0.999$  at both electrodes this shows the process is diffusion controlled at both electrodes with respect to  $\text{Ru}(\text{NH}_3)_6\text{Cl}_3$  probe. Nanoelectrode almost shows the same behavior with bare electrode except enhancement of current peak this may be due to overlapping of neighboring diffusion layers.

Graph of oxidation peak current of HQ vs scan rate overlapped in low scan rate and shows better proportionality when scan rate separated from 0.05 to 0.8  $\text{Vs}^{-1}$  and from 1.613 to 10 v/s at both bare GCE and nanohole PNA grafted GCE. This show diffusion controlled at low scan rate and fast mass transport at high scan rate.

A good linear relationship was observed between the anodic peak current and square root of the scan rate from 0.05 to 0.8  $\text{Vs}^{-1}$  with a correlation coefficient of  $R= 0.999$  and  $R = 0.998$  at nanohole NPA grafted GCE and bare GCE respectively, which shows the process is diffusion controlled at nanohole PNA grafted GCE and adsorption controlled at bare GCE at low scan rate.

Anodic peak current shows good relationship to square root of scan rate from 1.613 to 10 $\text{Vs}^{-1}$  with a correlation coefficient of  $R= 0.998$  and  $R = 0.995$  at nanohole PNA grafted GCE and at bare GCE respectively, which shows the process is diffusion controlled at nanohole PNA grafted GCE and adsorption controlled at bare GCE at high scan rate.

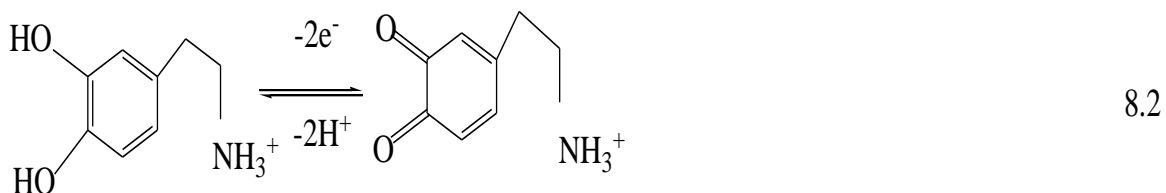
Table 7 Effect of scan rate on oxidation peak current of Ru(NH<sub>3</sub>)<sub>6</sub>Cl<sub>3</sub> and HQ at bare and nanohole p-nitroaniline grafted glassy carbon electrode.

Probes	Electrodes	Regression line fitted scan rate		Regression line fitted to square root of scan rate		Range of scan rate in v/s
		Equation	R	Equation	R	
Ru(NH <sub>3</sub> ) <sub>6</sub> Cl <sub>3</sub>	Bare GCE	Y = 0.05X + 0.08	0.962	Y = 0.17X + 0.02	0.999	0.05 to 10
	Nanohole PNA grafted GCE	Y = 0.07X + 0.11	0.970	Y = 0.24X + 0.03	0.999	
	Bare GCE	Y = 0.14X + 0.02	0.977	Y = 0.17X - 0.02	0.996	0.05 to 0.8
	Nanohole PNA grafted GC	Y = 0.19X + 0.03	0.991	Y = 0.22X - 0.02	0.999	
	Bare GCE	Y = 0.04X + 0.16	0.986	Y = 0.16X - 0.01	0.9971	1.613 to 10
	Nanohole PNA grafted GCE	Y = 0.53X + 0.21	0.988	Y = 0.24X - 0.04	0.9977	
HQ	Bare GCE	Y = 0.19X + 0.498	0.953	Y = 0.69X + 0.1	0.997	0.05 to 10
	Nanohole PNA grafted GCE	Y = 0.26X + 0.65	0.963	Y = 0.9X + 0.14	0.999	
	Bare GCE	0.64X + 0.23	0.983	Y = 0.74X + 0.056	0.9997	0.05 to 0.8
	Nanohole PNA grafted GCE	Y = 0.86X + 0.32	0.987	Y = 0.998X + 0.08	0.998	
	Bare GCE	0.14X + 0.87	0.978	Y = 0.63X + 0.23	0.995	1.613 to 10
	Nanohole PNA grafted GCE	Y = 0.196X + 1.1	0.986	Y = 0.87X + 0.22	0.998	



### 3.8.5 Cyclic Voltammetry of Dopamine

Nanohole PNA grafted GCE was applied for electroanalysis of dopamine because dopamine is electropositive analyte and its redox peak could be enhanced at ionic film modified electrode



As shown in fig.28 Oxidation peak current of DA enhanced at nanohole PNA grafted GCE relative to at bare GCE, which is attributed to 3D diffusion of ions toward nanohole electrode and electrostatic interaction between positively charged DA and negatively charged PNA film. Therefore nanohole PNA grafted GCE was used for electroanalysis of DA.

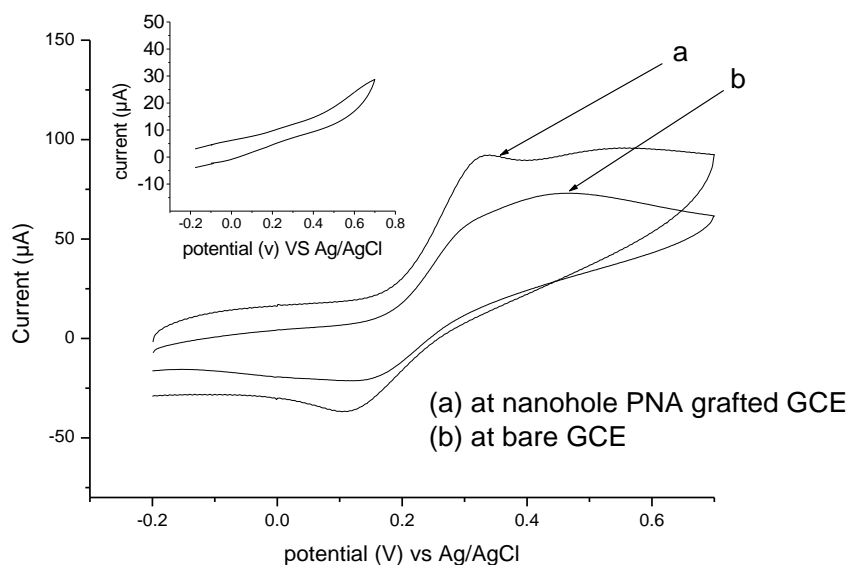


Figure 28. Cyclic voltamogram of 2 mmol/L DA in 0.1 mol/L sodium phosphate buffer (pH 7.5) at (a) nanohole PNA grafted GCE and (b) bare GCE; Inset Cyclic voltamogram of nanohole PNA grafted GCE in sodium phosphate buffer (pH 7.5), in all cases scan rate is 100 mV/s

It is known that DA is protonated in acidic media and hence develop positive charge therefore it is repelled by positive films 4-aminophenol and p-phenylenediamine. That is why its signal response is suppressed at nanohole APh grafted GC and nanohole PD grafted GCE.

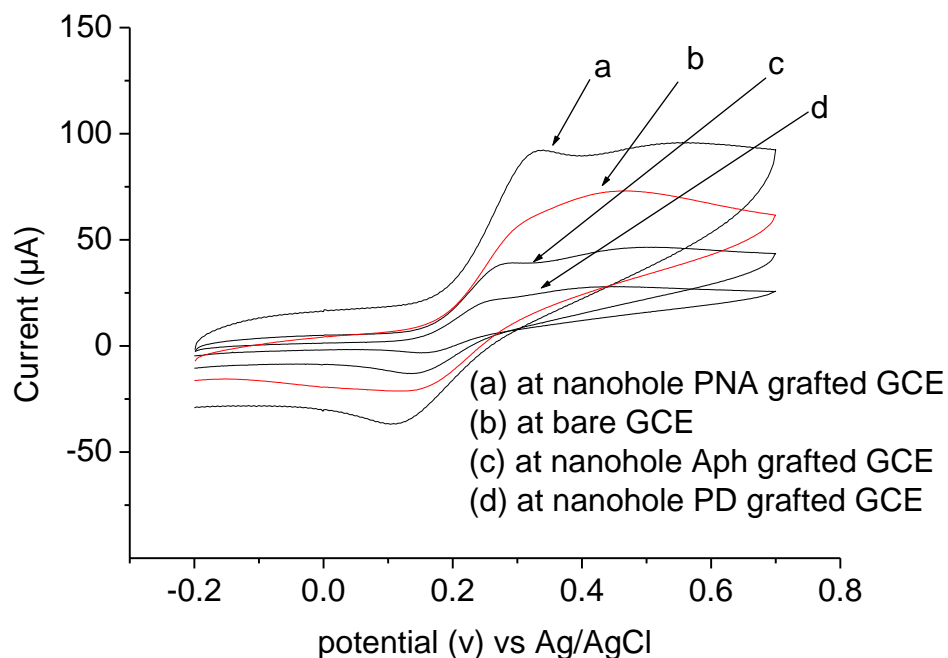
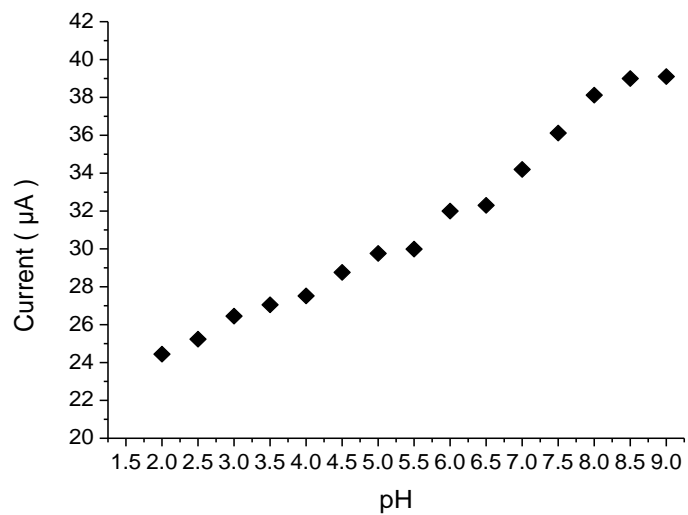


Figure 29. Cyclic Voltammogram of 2 mmol/L DA in 0.1 sodium phosphate buffer (pH 7.5) at (a) nanohole PNA grafted GCE (b) bare GCE (c) nanohole Aph grafted GCE (D) nanohole PD grafted GCE at scan rate of 100 mV/s in all cases.

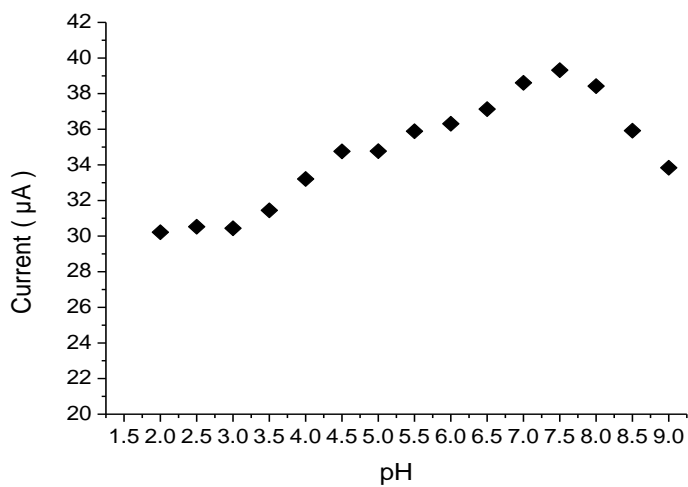
### 3.8.5.1 Effect of pH on Oxidation of Dopamine

Effect of pH of the supporting electrolyte (buffer) on oxidation of DA was studied with the range of 2 to 9. Citrate buffer was used to study effect of pH within the range of 2 to 4, acetate buffer was used within range of 4.5 to 6 and phosphate buffer was used within range of 6.5 to 9. As shown in Figure 30 oxidation peak current of DA increase from low to high pH; which shows oxidation of DA is favorable at high pH than at low pH due to proton transfer involved in oxidation of DA<sup>7, 50,106</sup>.

At nanohole PNA grafted GCE oxidation peak current increased with pH from pH 2 to 7 and reached its maximum at pH 7.5, this could be due to DA is readily pre-concentrated on negatively charged film formed on the electrode surface. This shows low pH neutralize some of the negative charge on the electrode surface and decrease attraction between film and DA which further decrease oxidation peak current of DA. When pH increased further beyond pH 7.5 oxidation peak current of DA decreased due to repulsion develop between negative charge on the electrode surface and hydroxide ions at high pH. Generally the modified electrode showed highest sensitivity at pH 7.5 but showed low sensitivity both in strong acid and base solutions and similar result was reported by Xiao et.al at pH 7.4<sup>111</sup>. Therefore 0.1 mol/L phosphate buffer solutions at pH 7.5 used as supporting electrolyte for electroanalysis of DA.



(i)

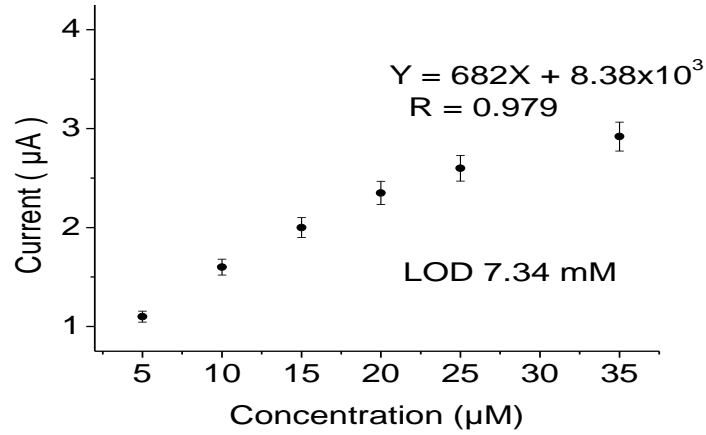


(ii)

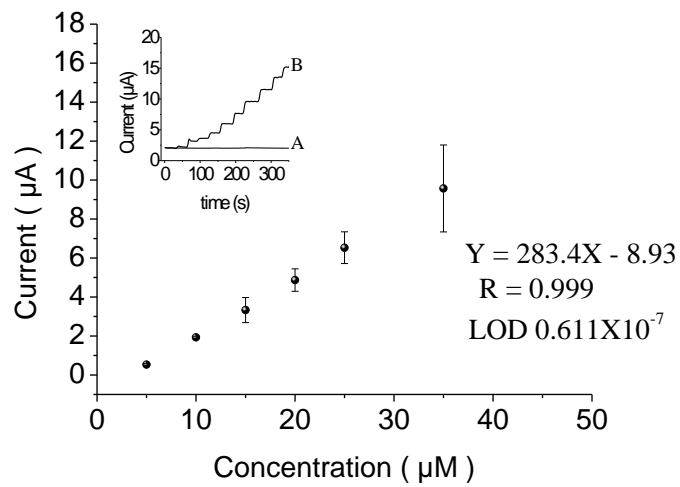
Figure 30. Plot of oxidation peak current of 2 mmol/L DA vs pH at (i) bare GCE and (ii) nanohole PNA grafted GCE in all cases scan rate 100 mV/s

### 3.8.5.2 Amperometric Response of Dopamine

Figure 31 displays amperometric response of DA at bare GCE and nanohole PNA grafted GCE. Amperometric study was carried out through successive addition of DA into a continuously stirred batch system of 0.1 mol/L phosphate buffer (pH 7.5) at applied potential of 0.8 V and 0.25 V at bare and nanohole PNA grafted GCE respectively. A linear relationship between oxidation peak current and concentration of DA was observed in the range from  $4 \times 10^{-4}$  to  $2.8 \times 10^{-5}$  with a coefficient of 0.979 and 0.999 at bare and nanohole PNA grafted GCE respectively, demonstrating good relationship between oxidation peak current and concentration. The limit of detection (LOD) at nanohole PNA grafted GCE and at bare GCE were 0.0611  $\mu\text{mol/L}$  and 7.34  $\text{mmol/L}$  respectively. The current values were the average of three measurements for each concentration. The limit of detection at nanohole PNA grafted GCE is improved relative to some other previous works<sup>112, 113</sup> (Table 8). These experimental results indicate that nanohole PNA grafted GCE has potential application as a good electrochemical sensor for the determination of DA.



(i)



(ii)

Figure 31. Calibration curve of amperometric response of DA at (i) bare GCE and (ii) nanohole PNA grafted GCE.; inset (A) amperometric response of phosphate buffer ( B) amperometric current vs time curve upon successive additions of 1 mol/L DA into a stirred system of 0.1 mol/L sodium phosphate buffer; (pH 7.5) in all cases.

### 3.8.5.3 Interference study

The major sources of interference in dopamine determination are common coexisting species in biological fluids which lead to overlap with redox peak current of dopamine<sup>114</sup>. The effect of ascorbic acid (AA), uric acid (UA), glucose (GLU) and tartaric acid (TA) on the amperometric peak response of 1 mmol/L of DA was examined. At bare GCE 1 mmol/L of each of these interferents found to give amperometric response the same as 1 mmol/L DA but it was observed that 100-fold concentrations of these possible interferents found to have no significant influence on the amperometric peak response of 1 mmol/L DA at nanohole PNA grafted GCE. This due to attraction of DA by p-nitroaniline negative film and repulsion of negative substance by the film at 0.25V

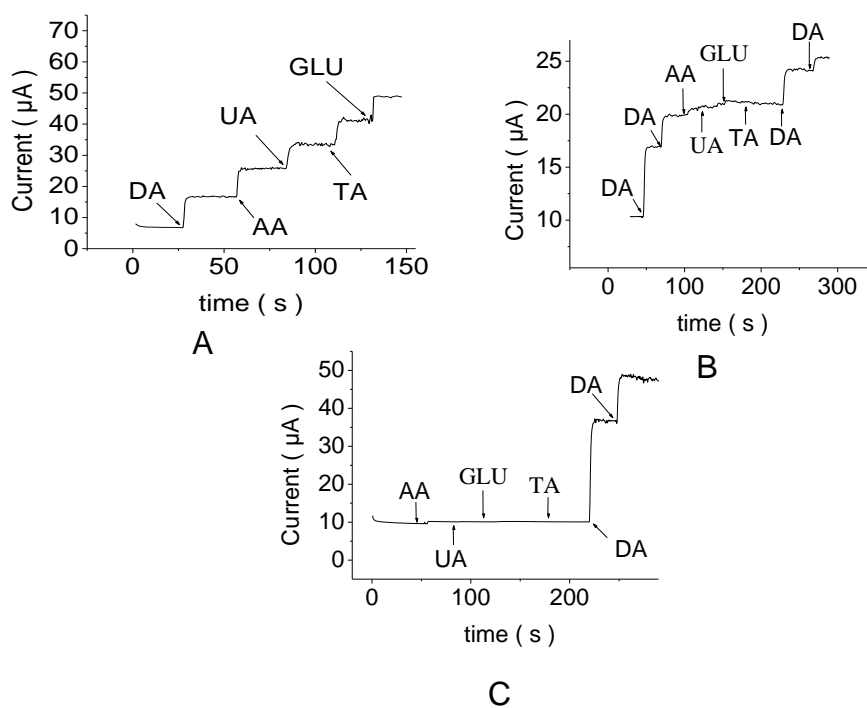


Figure 32. Amperometric responses of (A) 1 mmol/L DA and interfering species at (A) bare GCE at 0.8 V (B) 1 mmol/L DA and 200-fold excesses of interfering species at nanohole PNA grafted GCE and (C) amperometric response 200-fold excesses of interfering species and 1 mmol/L DA from interferent to DA at nanohole PNA grafted GCE. In all cases pH is 7.5

### **3.8.6 Stability and Reproducibility of Nanohole p-Nitroaniline Grafted Glassy carbon Electrode**

Five nanohole PNA grafted GCE were fabricated in different days under the same preparing conditions and the peak current of 2 mmol/L DA was measured at each electrodes. The relative standard deviation of peak current of these result was 5.27% (n=5), showing good reproducibility of the nanohole PNA grafted GCE. Nanohole PNA grafted GCE was prepared according to the optimized condition and stored in 0.1mmol/L phosphate buffer (pH 7.5) solution and the stability of modified electrode was tested on 28 days at 2mmol/L DA; the peak current of DA retained 97% of its initial current response. The result showed that nanohole PNA grafted GCE has a good stability and long life.



Table 8 Comparison of the Limit of Detection of the Fabricated Electrodes to Some Literatures

Sample Analyzed	New electrodes	Obtained data			Reported data	
		LOD in $\mu\text{mol/L}$	Dynamic range		Previous electrodes	LOD in $\mu\text{mol/L}$
			Concentration range in $\mu\text{mol/L}$	R		
AA	Nanohole Aph grafted GCE	0.626	5 to 45	0.994	Bi <sub>2</sub> O <sub>2</sub> Microparticles Modified Glassy Carbon Electrode <sup>104</sup>	8.1
	Nanohole PD grafted GCE	0.123	5 to 45	0.998	Tiron Modified Glassy Carbon Electrode <sup>105</sup>	1.79
DA	Nanohole PNA grafted GC E	0.0611	5 to 35	0.999	Overoxidized Polypyrrole/Graphene Modified Electrodes <sup>112</sup>	0.1
					Acrylamide Modified Carbon Paste Electrode <sup>113</sup>	0.35

#### **4 Conclusion and Future Prospective**

In this work fabrication and electrochemical characterization of three types of randomly nanoarrayed electrodes have been studied with exemplified application. The fabrication method presented could be generalized to produce nanoelectrode arrays of other metals provided that the electronucleation of metallic nanoparticles and effective insulating layer on carbon microspheres is obtained. The synthesized nanohole PD grafted GCE and nanohole APh grafted GC electrodes were found to have good characteristics for selective determination of ascorbic acid and might be used as a strategy for the selective determination of other electroactive negatively charged analytes where cationic species could interfere. Nanohole PNA grafted GCE was found to have good characteristics as for the sensing of dopamine hydrochloride and might be used as a strategy for the selective determination of other cationic electroactive substances where the anionic species interfere. Such nanoelectrode arrays can be employed for detecting different important trace samples in different field of studies.

## Reference

1. Christopher, M. A.; Ana, B. M. *Electrochemistry Principles, Methods, and Applications*. Oxford University Press: New York, 1993; Vol. 1.
2. Mazloum-Ardakani, M.; Beitollahi, H.; Ganjipour, B.; Naeimi, H.; Nejati, M. Voltammetric Determination of Dopamine at the Surface of TiO<sub>2</sub> Nanoparticles Modified Carbon Paste Electrode. *Bioelectrochemistry* **2009**, *75*, 2-4.
3. Xiao, L. F.; Chen, J.; Cha, C. S. Elimination of the interference of ascorbic acid in the amperometric detection of biomolecules in body fluid samples and the simple detection of uric acid in human serum and urine by using the powder microelectrode technique. *J. Electroanal. Chem.* **2000**, *495*, 27-35.
4. Ardakani, M.; Talebi, A.; Naeimi, H.; Barzoky, M.; Taghavinia, N. Fabrication of modified TiO<sub>2</sub> nanoparticle carbon paste electrode for simultaneous determination of dopamine, uric acid, and L-cysteine. *J. Solid State Electrochem.* **2009**, *13*, 1433.
5. Wang, B.; Zou, X.; Hong, D.M. Collard Photoinduced vibrational absorptions from poly(3 octylthiophene)/Fe<sub>2</sub>O<sub>3</sub> nanoparticle composite, a time-resolved FTIR study. *Synthetic Metals* **2000**, *113*, 223-226.
6. Han, M.; Cho, S.; Oh, S.; Im, S. Preparation and characterization of polyaniline nanoparticles synthesized from DBSA micellar solution. *Synthetic Metals*. **2002**, *126*, 53-60.
7. Martínez-Huitle, C. A.; Cerro-Lopez, M.; Antonio Quiroz, M. Electrochemical Behaviour of Dopamine at Covalent Modified Glassy Carbon Electrode with L-Cysteine: Preliminary Results. *Materials Research* **2009**, *12*, 375-384.
8. Fiorito, P.A.; Goncales, V.R.; Ponzio, E.A.; Torresi, S.I. Synthesis, characterization and immobilization of Prussian blue nanoparticles. A potential tool for bio sensing devices. *Chemical Communications*. **2005**, *3*, 366-368.
9. Minde, R.B.; Mallat, T.; Baiker, A.; Wang, G.; Heinz, T.; Pfaltz, A. A Novel Aminoalcohol Modifier for the Enantioselective Hydrogenation of Ethyl Pyruvate on Pt/Alumina. *Journal of Catalysis*. **1995**, *154*, 371-378.
10. Wang, J. Real-time electrochemical monitoring: toward green analytical chemistry. *Accounts of Chemical Research*. **2002**, *35*, 811-817.
11. Murray, R.W.; Bard, A.J.; Dekker, M. Chemically Modified Electrodes. *J. Electroanal. Chem.* **1984**, *13*, 191-368.

12. Murray, R. W. *Molecular Design of Electrode Surfaces*. J. Wiley & Sons: New York, 1992, p 22.
13. Mir, M.; Vreeke, M.; Katakis, I. Aptamers as elements of bioelectronic devices. *Electrochem. Commun.* **2006**, *8*, 505.
14. Gregory, S.; Torsten, R.; Burkhard, R. Nanoporous gold film encapsulating cytochrome for the fabrication of a H<sub>2</sub>O<sub>2</sub> biosensor. *J. Electroanal. Chem.* **2002**, *526*, 125.
15. Tesfaye, R.S.; Strutwolf, J.; O'Sullivan, C.K. Electrochemical Fabrication Nanostructured Surfaces for Enhanced Response. *Phys Chem.* **2008**, *9* 920 - 92.
16. Gooding, J. L.; Lai, L. H.; Ian, Y.; Goon, I.Y. *Nanostructured Electrodes with Unique Properties for Biological and Other Applications. Advances in Electrochemical Science and Engineering*. Weinheim: WILEY-VCH, 2009.
17. Moses, P. R.; Murray. R. W. Chemically modified tin oxide electrode *J. Anal. Chem.* **1975**, *47*, 1882.
18. Zoski, C. G. *Handbook of Electrochemistry*. Elsevier: Netherlands, 2007, p 295-297.
19. Elliott, C. M.; Murray, R. W. Chemically Modified Carbon Electrodes. *J. Anal. Chem.* **1976**, *48*, 1247.
20. Downard, A. J. Electrochemically Assisted Covalent Modification of Carbon Electrodes. *Electroanalysis.* **2000**, *12*, 1085-1096.
21. Deinhammer, R.; Ho, M.; Anderegg, M.; Porter, M.D. Electrochemical oxidation of amine-containing compounds: A route to the surface modification of glassy carbon electrodes. *Langmuir.* **1994**, *13*, 123.
22. Allongue, P.; Delamar, M.; Desbat, B.; Fagebaume, O.; Hitmi, R.; Pinson, K.; Saveant, J.M. Covalent Modification of Carbon Surfaces by Aryl Radicals Generated from the Electrochemical Reduction of Diazonium Salts. *J. Am. Chem. Soc.* **1997**, *119*, 201-207.
23. Arrigan, D. Nanoelectrodes, nanoelectrode arrays and their applications. *Analyst.* **2004**, *129*, 1157 - 1165.
24. Bernard, M.; Chausse, A.; Cabet-Deliry, E.; Chehimi, M.; Pinson, J.; Podvorica, F.; Vautrin-Ul, C. The formation of covalently bonded organic layers and their effect on corrosion. *Chem. Mater.* **2003**, *15*, 3450.
25. Fitch, A. Clay-modified electrodes. *Clays and Clay Minerals.* **1990**, *38*, 391-400.
26. Qu, D. Investigation of oxygen reduction on activated carbon electrodes in alkaline solution. *Carbon.* **2007**, *45*, 1296-1301

27. Ojani, R.; Raoof, J.B.; Rahemi, V. A Simple and Efficient Electrochemical Sensor for Electrocatalytic Reduction of Nitrite Based on Poly(4-aminoacetanilide) Film Using Carbon Paste Electrode. *J. Chin. Chem. Soc.* **2011**, *58*, 247-254.
28. Pournaghi-Azar, M.H.; Ojani, R. Electrochemistry and electrocatalytic activity of polypyrrole/ferrocyanide films on a glassy carbon electrode. *J. Solid State Electrochem.* **2000**, *4*, 75-79.
29. Casella, I.G.; Guascito, M.R. Electrocatalysis of ascorbic acid on the glassy carbon electrode chemically modified with polyaniline films. *Electroanalysis.* **1997**, *9*, 1381-1386.
30. Mao, H.; Pickup, P.G. Electronically conductive anion exchange polymers based on polypyrrole: Preparation, characterization, electrostatic binding of ferrocyanide and electrocatalysis of ascorbic acid oxidation. *J. Electroanal. Chem.* **1989**, *265*, 127-142.
31. Gooding, J.J.; Hibbert, D.B. The application of alkanethiol self-assembled monolayers to enzyme electrodes. *Trends Anal. Chem.* **1999**, *18*, 525.
32. Švancara, I.; Hradilová, Š.; Nepejchalová, L.; Bartoš, I.; Metelka, R. Carbon paste electrodes in electroanalytical chemistry. *J. Serb. Chem. Soc.* **2009**, *74*, 1021-1033
33. Kuwana, T.; French, W. G. Carbon paste electrodes containing some electroactive compounds. *J. Anal. Chem.* **1964**, *36*, 241.
34. Ravichandran, K. Baldwin, R. P. Chemically Modified Carbon Paste Electrodes in Voltammetric Analysis. *J. Electroanal. Chem.* **1981**, *126*, 293-300.
35. Kalcher, G.; Scanvangaer, V.; Bizuk, M.; Vytras, K.; Walcarius, A. Electrochemical sensors and biosensors based on heterogeneous carbon materials. *Monatsh.* **2009**, *140*, 861-889.
36. Finot, M.; McDermot, M. Characterization of *n*-alkanethiolate monolayers adsorbed to electrochemically deposited gold nanocrystals on glassy carbon electrodes. *J. Electroanal. Chem.* **2000**, *488*, 125-132.
37. Fan, F.; Yao, Y.; Cai, L.; Cheng, L.; Tour, J.; Bard, A. J. Structure-Dependent Charge Transport and Storage in Self-Assembled Monolayers of Compounds of Interest in Molecular Electronics: Effect of Tip Material, Head Group and Surface Concentration. *J. Am. Chem. Soc.* **2004**, *126*, 4035-4042.
38. Polsky, R.; Gill, R.; Kaganovsky, L.; Willner, I. Amplified Transduction of Biomolecular Interactions Based on the Use of Nanomaterials. *Anal. Chem.* **2006**, *78*, 2268.
39. Mirkin, V.; Fan, F.; Bard, A. Evaluation of the tip shapes of nanometer size microelectrodes. *J. Electroanal. Chem.* **1992**, *328*, 47.

40. Ugo, P.; Moretto, L.; Vezza, F. *Direct electroanalysis of proteins at nanoelectrode ensembles. Phys Chem.* **2002**, *3*, 917.
41. Penne, R.M.; Martin, C.R. Preparation and Electrochemical Characterization of Ultramicroelectrodes Ensembles. *J. Anal.Chem.* **1987**, *59*, 2625.
42. Menon, V. P.; Martin, C.R. Fabrication and evaluation of nanoelectrode ensembles. *J. Anal. Chem.* **1995**, *67*, 1920-1928.
43. Creager, S.E.; Radford, P.T. Electrochemical reactivity at redox molecule based nanoelectrode ensembles. *J. Electroanal. Chem.* **2001**, *500*, 21.
44. Schotter, M.; Bal, A.; Ursache, M.;Tuominen, C.; Stafford, T.; Russell, V.; Rotello, M. Fabrication and characterization of nanoelectrode arrays formed via block copolymer self-assembly. *Langmuir.* **2001**, *17*, 6396-6398.
45. Evans, U.; Colavita, P.; Doescher, M.; Schiza, M.; Myricks, M. Construction and Characterization of a Nanowell Electrode Array. *Nano Lett.* **2002**, *2*, 641.
46. Doescher, M.S.; Evans, U.; Colavita, P. E.; Miney, P. G.; Myrick, M. L. Construction of a nanowell electrode array by electrochemical gold stripping and ion bombardment. *Electrochemical and Solid State Letters.* **2003**, *6*, 112-C115.
47. Koehne, J.; Li, J.; Cassell, A.; Chen, H.; Ye, H.; Ng, T.; Han, J.; Meyyappan, M. The fabrication and electrochemical characterization of carbon nanotube nanoelectrode arrays. *J Mater Chem.* **2004**, *14*, 676-684.
48. Wilson, M. S. Electrochemical immunosensors for the simultaneous detection of two tumor markers. *Anal. Chem.* **2005**, *77*, 1496.
49. Nassef, M.H.; Radi, A.d.; OSullivan, C. Electrocatalytic oxidation of hydrazine at o-aminophenol grafted modified glassy carbon electrode: reusable hydrazine amperometric sensor. *J. Elect. Chem* **2006**, *592*, 139-146.
50. Badia, A.; G. W.; Singh, S.; Demers, L.; Cuccia, L.; Reven, L. Structure and Chain Dynamics of Alkanethiol-Capped Gold Colloids. *Langmuir.* **1996**, *12*, 1262-1269.
51. Sun, X.; Jiang, X.; Dong, S.; Wang, E. One-Step Synthesis and Size Control of Dendrimer-Protected Gold Nanoparticles. *A Heat-Treatment-Based Strategy* **1997**, *32* 1242-1249.
52. Marken, F.; Compton, R.G.; Buston, J.; Moloney, M. The Pb(IV) catalyzed cleavage of 1,2-cis-cyclopentanediol at graphite and glassy carbon electrodes. *Electroanalysis.* **1998**, *10*, 1188-1192.

53. Tseng, A.; Notargiacomo, A.; Chen, T. Nanofabrication by scanning probe microscope lithograph. *Journal of Vacuum Science & Technology*. **2005**, *23*, 877-894.
54. Tang, C.; Tian, G.; Wang, Y.; Su, Z.; Li, C.; Lin, B.; Huang, H.; Yu, X.; Li, X.; Long, Y.; Zeng, Y. Selective response of dopamine in the presence of ascorbic acid and uric acid at gold nanoparticles and multi-walled carbon nanotubes grafted with ethylene diamine tetraacetic acid modified electrode. *Bull. Chem. Soc. Ethiop.* **2009**, *23*, 317-326.
55. Lyons, M.; Breen, W.; Cassidy, J. Ascorbic acid oxidation at polypyrrole-coated electrodes. *J. Chem. Soc. Faraday Trans.* **1991**, *87*, 115-123.
56. Heien, A.V.; Khan, A.S.; Ariansen, J. L.; Cheer, J.S.; Phillips, E.M.; Wassum, K. M.; Wightman, R. M. Real-time measurement of dopamine fluctuations after cocaine in the brain of behaving rats. *Proc. Natl. Acad. Sci.* **2005**, *102*, 10023. .
57. Wightman, R.M. May, L. J.; Michael, A. C. Detection of Dopamine Dynamics in the Brain *Anal. Chem.* **1988**, *60* 769.
58. Foster, K.; McCormac, T. Electrochemical properties of an osmium (ii) copolymer film and its electrocatalytic ability towards the oxidation of ascorbic acid in acidic and neutral pH. *Electroanalysis*. **2006**, *18*, 1097-1104.
59. Zeng, Y.L.; Li, C. X.; Tang, C. R.; Zhang, X. B.; Shen, G. L.; Yu, R. Q. The electrochemical properties of Co (TPP), tetraphenylborate modified glassy carbon electrode: application to dopamine and uric acid analysis. *Electroanal.* **2006**, *18*, 440- 448.
60. Zhao, H.; Zhang, Y.; Yuan, Z. Electrochemical determination of dopamine using a poly(2-picolinic acid) modified glassy electrode. *Analyst*. **2001**, *126*, 358-360.
61. Downard, A.J.; Roddick, A.D.; Bond, A.M. Covalent bond modification of carbon electrodes for voltammetric differentiation of dopamine and ascorbic acid. *Analytica Chimica Acta*. **1995**, *317*, 303-310.
62. Mazloum-Ardakani, M.; Beitollahi, H.; Ganjipour, B.; Naeimi, H.; Nejati, M. Voltammetric Determination of Dopamine at the Surface of TiO<sub>2</sub> Nanoparticles Modified Carbon Paste Electrode. *Bioelectrochemistry*. **2009**, *75*, 2-4.
63. Alderman, M.; Aiyer, K.J. Uric acid: role in cardiovascular disease and effects of losartan. *Curr. Med. Res. Opin.* **2004**, *20*, 369.
64. Lindy, M. Biosensors and bioelectrochemistry. *Curr Opin Chem Biol.* **2006**, *10*, 177.

65. Lupu, S.; Mucci, A.; Pigani, L.; Seeber, R.; Zanardi, C. Polythiophene derivative conducting polymer modified electrodes and microelectrodes for determination of ascorbic acid. effect of possible interferents. *Electroanalysis* **2002**, *14*, 519-525.
66. Zhao, H.; Zhang, y.; Yuan, Z. Study on the electrochemical behavior of dopamine with poly(sulfosalicylic acid) modified glassy carbon electrode. *Analytica Chimica Acta*. **2001**, *441*, 117-122.
67. Li, J.; Lin, X. Simultaneous determination of dopamine and serotonin on gold nanocluster/overoxidized-polypyrrole composite modified glassy carbon electrode. *Sensors and Actuators* **2007**, *124*, 486-493.
68. Malem, F.; Mandle, D. Self Assembled Monolayers in Electroanalytical Chemistry: Application of Mercapto Carboxylic Acid Monolayers for the Electrochemical Detection of Dopamine in the Presence of a High Concentration of Ascorbic Acid. *J. Anal. Chem.* **1993**, *65*, 37-41.
69. Bond, A.M.; Oldham, K.B.; Zoski, C.G. Steady State Voltammetry. *Anal. Chim. Acta*. **1989**, *216*, 177-230.
70. Barek, J.; Fogg, A. G.; Muck, A.; Zima, J. Polarography and Voltammetry at Mercury Electrodes. *Critical Reviews In Analytical Chemistry*, **2001**, *31*, 291-309.
71. Bard, A. J.; Faulkner, L. R. *Electrochemical Methods: Fundamentals and Applications*. In Wiley Inc: United States of America, 2001: p833.
72. Wang, J. *Analytical Electrochemistry*. A John Wiley and sons: New York, Vol. 2nd edition, 2001: p29
73. Faulkner, L.R.; Bard, A. J. *Basic Potential Step Methods, Electrochemical Methods*: New Jersey: Wiley, 2000: p156-225.
74. Noroozifar, M.; Motlagh, M.K. Solid-phase iodine as an oxidant in flow injection analysis:determination of ascorbic acid in pharmaceuticals and foods by background correction. *Talanta*. **2003**, *61*, 173-179.
75. Shrivastava, S. Nanofabrication for drug delivery and tissue engineering. *Digest Journal of Nanomaterials and Biostructures* **2008**, *3*, 257-263.
76. Meriaudeau, F.; Downey,T.; Passian, A.; Wig, A.; Ferrell, T. L. Environment Effects on Surface-Plasmon Spectra in Gold-Island Films Potential for Sensing Applications. *Appl. Opt.* **1998**, *37*, 8030-8037.



77. Ng, W.; Wu, L.; Moran, P. Microcontact printing of catalytic nanoparticles for selective electroless deposition of metals on nonplanar polymeric substrates. *Appl. Phys. Lett.* **2002**, *81*, 3097- 3099.
78. Brust, M.; Bethell, D.; Schiffrin, D. J.; Kiely, C. J. Novel Gold-Dithiol Nano-Networks with Non-metallic Electronic Properties. *Adv. Mater.* **1995**, *7*, 795.
79. Korgel, B. A.; Fitzmaurice, D. condensation of ordered nanocrystal thin films *Phys. Rev. Lett.* **1998**, *80*, 3531-3534.
80. Kozuka, H.; Sakka, S. Preparation of gold colloid-dispersed silica coating films by the sol-gel method. *Chem. Mater.* **1993**, *5*, 222-228.
81. Decher, G.;Eckle, M.; Schmitt, J.; Struth, B. Layer-by-layer assembled multilayer films *Curr. Opin. Colloid Interface Sci.* **1998**, *3*, 32-39.
82. Navani, N.; Li, Y. Nucleic acid aptamers and enzyme as sensor. *Opin.Chem.Biol.* **2006**, *10* 272.
83. Tuerk, C.; Gold, L. Systematic evolution of ligands by exponential enrichment RNA ligands to bacteriophage T<sub>4</sub> DNA polymerase. *Science.* **1990**, *249*, 505-510.
84. Li, T.; Fu, R.; Park. H. Pyrrolo-dC based fluorescent aptasensors for the molecular recognition of targets. *chemical communications.* **2010**, *46*, 3271-3273
85. Brainina, K.; Malakhova, N.A.; Stojko, Y. Stripping Voltammetry in Environmental and Food Analysis. *J Anal Chem.* **2000**, *368*, 307-325.
86. Bond, A.M. Past, present and future contributions of microelectrodes to analytical studies employing voltammetric detection. *Analyst.* **1994**, *119*, 1-21.
87. Wightman, R. M.; Wipf. D. O. Voltammetry at Ultramicroelectrodes *In Electroanalytical Chemistry*; Bard, A. J., Ed.; Marcel Dekker: New York, 1988: V. 15, p267-353.
88. Penner, R.M.; Heben, M. J.; Longin, T. L.; Lewis, N. S. Fabrication and use of nanometer-sized electrodes in electrochemistry. *Science.* **1990**, *250*, 1118.
89. Pandey, P.; Dattab, M.B.; Malhotra, B. D. Prospects of Nanomaterials in Biosensors. *Analytical Letters* **2008**, *41*, 159 - 209.
90. Zoski, C.G. Ultramicroelectrodes: Design, Fabrication, and Characterization. *Electroanalysis* **2002**, *14*, 1041-1051.
91. DeIamar, M.; Hitmi, R.; Pinson, J.; Savéant, J. Complete conversion of L-lactate into D-lactate. A generic approach involving enzymatic catalysis, electrochemical oxidation of NADH and electrochemical reduction of pyruvate. *J. Am. Chem. Soc.* **1992**, *114*, 5883.

92. Bockris, J. O.; Bockris, J.O.; Khan, S.U. *Surface Electrochemistry: A Molecular Level Approach*. Plenum Press: New York, 1993.
93. Kutter, J.; Geschke, O.; Klank, H.; Tellema, P. *Microfluidics: Theoretical Aspect in microsystem engineering of lab on chip devices*. Wiley, VCH: 2004: p452.
94. Lyskawa, J.; Belanger, D. Direct Modification of a Gold Electrode with Aminophenyl Groups by Electrochemical Reduction of in Situ Generated Aminophenyl Monodiazonium Cations. *Chemistry of Materials* **2006**, *18*, 4755-4763.
95. Baranton, S.; Belanger, D. Electrochemical Derivatization of Carbon Surface by Reduction of in Situ Generated Diazonium Cations. *J. Phys. Chem. B* **2005**, *109*, 24401-24410.
96. Arvand, M.; Sohrabnezhad, Sh.; Mousavi, M.F.; Shamsipur, M.; Zanjanchi, M.A. Electrochemical study of methylene blue incorporated into mordenite type zeolite and its application for amperometric determination of ascorbic acid in real samples. *Analytica Chimica Acta* **2003**, *491*, 193-201.
97. Mendham, J. D., R.C.; Barnes, J.D.; Thomas, M. *Vogel's*. Pearson Education: Singapore, 1998: 6th edition, p428-434.
98. Cruickshank, A.C.; Tan, E.S.; Brooksby, P.A.; Downard, A.J. Are Redox Probes a Useful Indicator of Film Stability? An Electrochemical, AFM and XPS Study of Electrografted Amine Films on Carbon. *Electrochemistry Communications*. **2007**, *9*, 1456-1462.
99. Saby, C.; Ortiz, B.; Champagne, G.Y.; Belanger, D. Electrochemical Modification of Glassy Carbon Electrode Using Aromatic Diazonium Salts .1. Blocking Effect of 4-Nitrophenyl and 4-Carboxyphenyl Groups. *Langmuir*. **1997**, *13*, 6805-6813.
100. Mévellec, V.; Roussel, S.; Tessier, L.; Chancelon, J.; Hermite, M.M.L.; Deniau, G.; Viel, P.; Palacin, S. Grafting Polymers on Surfaces: A New Powerful and Versatile Diazonium Salt-Based One-Step Process in Aqueous Media. *Chem. Mater.* **2007**, *19*, 6323-6330.
101. Zhang, M.; Gong, K.; Zhang, H.; Mao, L. Layer-by-layer assembled carbon nanotubes for selective determination of dopamine in the presence of ascorbic acid. *Biosensors and Bioelectronics* **2005**, *20*, 1270-1276.
102. Compton, R. G.; Henstridge, M. C.; Dickinson, E. J. F.; Aslanoglu, M.; McAuley, C. B. Voltammetric selectivity conferred by the modification of electrodes using conductive porous layers or films: The oxidation of dopamine on glassy carbon electrodes modified with multiwalled carbon nanotubes. *Sensors and Actuators*. **2010**, *145*, 417-427.

103. Nezamzadeh, A.; Amini, M. K.; Faghihian, H. Square-Wave Voltammetric Determination of Ascorbic Acid Based on its Electrocatalytic Oxidation at Zeolite-Modified Carbon-Paste Electrodes. *Int. J. Electrochem. Sci.* **2007**, *2*, 583 - 594.
104. Zidan, M.; Tee, T.W.; Abdullah, A.H.; Zainal, z.; Kheng, K.J. Electrochemical Oxidation of Ascorbic Acid Mediated by Bi<sub>2</sub>O<sub>3</sub> Microparticles Modified Glassy Carbon Electrode. *Int. J. Electrochem. Sci.* **2011**, *6*, 6289 - 300
105. Ensafi, A.A.; Taei, M.; Khayamian, T. Simultaneous Determination of Ascorbic Acid, Dopamine, and Uric Acid by Differential Pulse Voltammetry using Tiron Modified Glassy Carbon Electrode. *Int. J. Electrochem. Sci.* **2010**, *5*, 116 – 130
106. Razmi, H.; Harasi, M. Voltammetric Behavior and Amperometric Determination of Ascorbic Acid at Cadmium Pentacyanonitrosylferrate Film Modified GC Electrode. *Int. J. Electrochem. Sci.* **2008**, *3*, 82 - 95.
107. Sun, H.; Lain, K.; Liang, S.; Liu, Z. Preparation of activated rough electrode in KMnO<sub>4</sub> solutions and its application for the electrocatalytic oxidation of ascorbic acid. *Chemical Journal on Internet.* **2004**, *6*, 65.
108. Jafar, H.K.; Kazem, A.M.; Hamideh, G.; Shahra, T. Flow-Injection Amperometric Determination of Ascorbic Acid Using a Graphite-Epoxy Composite Electrode Modified with Cobalt Phthalocyanine. *Iran. J Chem. & Chem. Eng.* **2000**, *20*, 2.
109. Pisoschi, A. M.; Danet, A.F.; Kalinowski, S. Ascorbic Acid Determination in Commercial Fruit Juice Samples by Cyclic Voltammetry. *Journal of Automated Methods and Management in Chemistry* **2008**, *8*, 1-8.
110. Chairam, S.; Sriraksa, W.; Amatongchai, M.; Somsook, E. Electrocatalytic Oxidation of Ascorbic Acid Using a Poly(aniline-co-m-ferrocenylaniline) Modified Glassy Carbon Electrode. *Sensors and Actuators.* **2011**, *11*, 10166-10179.
111. Xiao, Y.; Guo, C.; Li, M.C.; Li.; Zhang, J.; Xue, R.; Zhang, S. Highly sensitive and selective method to detect dopamine in the presence of ascorbic acid by a new polymeric composite film. *J. Anal. Biochem.* **2007**, *371*, 229.112.
112. Zhuang, Z.; Li, J.; Xu, R.; Xiao, D. Electrochemical Detection of Dopamine in the Presence of Ascorbic Acid Using Overoxidized Polypyrrole/Graphene Modified Electrodes. *Int. J. Electrochem.* **2011**, *6*, 2149 - 2161

113. Shankar, S.S.; Swamy, B.E.K.; Pandurangachar, M.; Chandra, U.; Chandrashekar, B.N.; Manjunath, J.G.; Sherigara, B.S. Electrocatalytic Oxidation of Dopamine on Acrylamide Modified Carbon Paste Electrode : A Voltammetric Study. *Int. J. Electrochem. Sci.* **2010**, *5*, 944 - 954
114. Goyal, R. N.; Gupta, V.K.; Bachheti, N.; Sharma, R. A. Electrochemical Sensor for the Determination of Dopamine in Presence of High Concentration of Ascorbic Acid Using a Fullerene-C60 Coated Gold Electrode. *Electroanalysis.* **2008**, *20*, 757-764.